参考文献

Hiroi, T. et al., (1985) : A method to determine mineral assemblage of asteroidal surfaces by their spectral references –29 Amphitrite as an example of applications-, Proceedings of the 18th ISAS Lunar and Planetary Symposium, p.52-53.

Hiroi, T. and Takeda, H. (1989) : A method of converting reflectance spectra into absorption coefficient spectra of mineral mixtures for application to asteroidal surface mineralogy, Lunar and Planetary Science.

Hiroi, T. and Pieters, C. M. (1992) : Effects of grain size and shape in modeling reflectance spectra of mineral mixtures, Proceedings of Lunar and Planetary Science, Vol. 22, p.312-325.

金属鉱業事業団・(財)資源・環境観測解析センター (1995) : 平成 6 年度 資源衛星データ解析技術開発 報告書.

金属鉱業事業団・(財)資源・環境観測解析センター (1996) : 平成 7 年度 資源衛星データ解析技術開発 報告書.

斎藤元也・村上拓彦・石塚直樹・熊谷樹一郎・加藤雅胤・川上 亨・塚田 靖・俣野米治・飯田幸平 (1998) : ASTER データによる衛星土壌図の作成手法開発, (社)日本リモートセンシング学会, 第 24 回学術講演会論文集, p.147-150.

三箇智二・春山純一・大竹真紀子・大嶽久志 (1998) : 広域モザイク画像作成のための幾何補正手法と輝度補正法の開発－クレメンタイン探査機による月面画像への応用－, 情報地質, 第 9 巻, 第 3 号, p.135-145.

通商産業省・資源エネルギー庁 (1996) : 金属鉱物資源探査のための JERS-1 データ使用マニュアル, 鉱物資源探査技術開発調査・資源衛星による探査技術開発総括報告書, pp. 233.

あとがき

航空機に搭載されたカメラで撮影した写真を立体視し，地質・地質構造を判読する技術は，第二次大戦後から応用され始めたが，数100 kmの高い高度から撮像された衛星データの利用は穀物収穫量の把握を目的とした陸域観測用のランドサット1号が打ち上げられた1972年に始まり，ようやく26年が経過したに過ぎない。

人工衛星のセンサは第1世代のMMS，第2世代のTM，そして高い地表分解能と立体視機能を有する第3世代のHRVと進展してきている。1992年2月に打ち上げられた我が国のJERS-1(「ふよう1号」)には，立体視機能をもつ光学センサ(OPS)と合成開口レーダ(SAR)が搭載されており，いわばフル装備の資源探査衛星といえる。

MSS画像を通して人類が初めて宇宙空間から地球表面を直接観察できるようになった時の従来の認識に対するインパクトは計り知れないものがあった。衛星データの最大の武器は，広域性，同時性，客観性および回帰性であり，ディジタルデータでもあるため，スペクトル分解能の高いTMやOPSのデータは，コンピュータ処理によって現在では地球科学のあらゆる分野において各種の分類や強調処理などで応用されている。

金属鉱床探査の基礎的アプローチは，まず，実際の現地を踏査し，鉱床の生成に密接に関連する変質帯を詳細に記載し，試料を採取してそれらの変質帯の性格や鉱物組合せを知ることから始まる。現地の調査方法では，時代の変遷と共に，GPSや携帯用のスペクトルメータを使用するなどの多少の近代化が見られるものの，標高の高い山岳地帯や熱帯雨林のジャングル内をくまなく歩いて地表のデータを得るという基本的な方法は，昔も今もほとんど変わっていない。

しかしながら，近年，スペクトル分解能の高い航空機データや衛星データが取得できるようになってからは，これらの踏査に先立って，それらのデータを使用したヴィジュアルな詳細地質判読やコンピュータによる複雑な計算処理を行って，かなりの精度で定量的な鉱物判定をする解析が可能になりつつある。それらの室内解析の結果を十分に参考にすれば，時間，コストや労力・忍耐力を多大に要する地表踏査(わけても，アクセスの困難な地域について)を合理的に軽減させることができるといえよう。

上述の現状からみて，衛星画像や航空写真を用いた写真地質判読やコンピュータを使用したディジタル処理・解析によって，広大な対象地域から有用で多量な地質・地形情報が迅速に抽出されるということはコストに対する効果の大きい手法であろう。このようなメリットを考慮し，露岩地帯のみならず植生が密に繁茂する地域に対しても，精度の低い地形図の代替物としての基本図の役割のみならず，金属鉱床探査の予察調査として今後も航空機データや衛星データを活用することが望ましいと思料する。

巻　末　資　料

巻末資料 1　　抽出された変質帯の対比表 (LANDSAT TM 画像と JERS-1 OPS 画像)

巻末資料 2　　アルゼンティンにおける衛星画像解析結果の報告資料およびリモートセンシング・セミナーの講義資料

巻末資料 1　　抽出された変質帯の対比表 (LANDSAT TM 画像と JERS-1 OPS 画像)

Alteration

Number of Alteration	Lithology observed	Dimension (km)	Elongation	Intensity of alteration*	Structure Texture	Alteration Mineralogy mapped by JERS-1 OPS data	Prospect included
AA6025	Miv	8X2.5		2	lineament (NNE-SSW, NNW-SSE)		Veradero Sur
AA6026	Miv	3X3		2			Los Desdoblados
AA6027	Miv	2X1		2	Intrusive		
AA6028	Miv	1.5X1		2			
AA6030	Ps/Triv	7.5X4		2	lineament (NNW-SSE)		Cerro Colorada, Veladero Centro
AA6031	Ps/Triv	6X3		2			
AA6032	γp, Ps/Triv	18X5		2	lineament (N-S)	In northern central, Kao zone is located with small Alu zone in the NW, Alu zones are distributed in four zones at the northern area and four Ser zones are scattered in north east end and west edge of northern central area	La Ortiga
AA6033	γp	6X3		2			Nevada (Chile), Lama
AA6035	γp	2.5X0.5	N-S	2			Los Amarillos
AA6036	γp	12X3	NNW-SSE	2	lineament (N-S)		Manifestation NN
AA6037	γp	2.5X1.5		2		Kao predominates in the west and Alu predominates in the east	
AA6038	Mim, γt	4.5X1.5		2	lineament (NNW-SSE)	Small Kao zone is located at the north end with very small Alu zone while Alu zone with small Ser and Kao zone is located in the south	
AA6043	Mim	2X1		1		Long narrow Alu zone is located in N-S direction, surrounded by three Kao zones and Ser zone in the peripheral	
AA6045	Mim	0.5X0.5		1	argillitic intrusive or playa		
AA6047	Ps/Triv	1.5X1.5		2	lineament (N-S)	Kao area predominates in central and surrounded by Ser zone. Small Alu zone is located in the south end	
AA6048	Mim	1.5X0.5		1	playa (?)		
AA6051	γp, OlMiv	6X5		1		Alu zones are distributed in 6 zones, one in northern edge is along with small Kao and Ser zone, small Kao area is located besides second one from north	
AA6052	OlMiv	1.5X0.5		1		Alu predominates	
AA6053	Ol/OlMiv	2X1		2	lineament (NW-SE)	Alu predominates in northern part while Ser predominates in southern area	Rio de la Flecha
AA6054	γt	1.5X0.5		2	lineament (NNE-SSW)	Kao predominates and Ser zone is located in eastern edge	
AA6055	Ol/OlMiv	8.5X1.5	NE-SW	2		Three zones are distributed. Kao area is surrounded by Ser in the east and surrounded by Alu in the west, while the other is pure Kao zone	Carachas alteration
AA6056	γt	1.5X0.5	NE-SW	2	Intrusive	Alu zone is surrounded by Kao, Ser zone is located in the western edge	Cerro Amarillo
AA6057	Ol/OlMiv	0.5X0.5		2	circular structure, lineament (NE-SW)	Ser is distributed in the NE edge in NW-SE direction	
AA6058	γp	4X1.5		2		Alu predominates in northern area and Kao predominates in southern area	Los Mogotes
AA6059	γp	1.5X1		2	lineament (ENE-WSW)	Ser predominates in center	Ranchillos
AA6060	Cs	3X1.5		2		Ser zones are distributed besides Goe zones	Las Sapitos
AB6001	DC	0.5	N-S	1	N-S		Umango
AA6063	γp,OlMiv	9X2.5		2		Zonal distributions of Alu in northern central and Kao in southern central, small zone of Kao in northern edge and those of Kao and Alu in western area	El Potoro

Alteration

Number of Alteration	Lithology observed	Dimension (km)	Elongation	Intensity of alteration*	Structure Texture	Alteration Mineralogy mapped by JERS-1 OPS data	Prospect included
AA6064	γp,OlMiv	3X1.5		2	lineament (NE-SW)	Zonal distribution of Kao in northern area	
AA6065	Ol/OlMiv	3.5X1		1	lineament (NE-SW)		
AA6066	Qv	2X1.5		2		Kao predominates in southern area and small Alu areas are distributed in northern edge	Rio Blanco
AA6067	Qv	1X0.5		2	Intrusive	Kao predominates while small Ser zone in center and Alu zone in western edge	
AA6068	γp,Tv	20X5.5	NE-SW	2	lineament (N-S)	Kao predominates in several scattered areas in center, Alu and Ser zone is distributed in north-eastern and western area	Cerro Colorada, La Olita
AA6073	Cs	5X1	NNE-SSW	2	lineament (NE-SW)	Clear Alu zone in northern edge, Ser and Alu areas are distributed in southern area	Carnerito
AA6074	Cs	1X0.5		2			
AB7001	Ds	1.5X0.5	NE-SW	2	lineament (NNW-SSE)		
JE101	ρt	7.5X5	N-S	2	lineament (N-S)	Kao predominates in most of the area	Rio Frio
AA7043	γp,Olmiv	4X3.5	E-W	2		Kao predominates in most of the area and Ser zones are located in north- and west-end	Del Carmen (Carmen
JE102	γp	4X1	N-S	2		Kao predomonates the area with Ser fringe, Alu appeares at NE corner	
JE103	γp	6X2.5	N-S	2		Kao predominates the area with Ser fringe	
JE104	γp	1.5X0.5	NW-SE	1		Kao predominates	
JE105	γp	1.5X1	N-S	1		Kao predominates	
AA7046	γp,Of	2X1.5	E-W	0.5			
AA7047	γp	3.5X2	N-S	0.5			
AA7049	γp	9X3	NNW-SSE	1			Las Openas
AA7050	CPb	2X1.5	E-W	1		Kao predominates in central with very small Alu zones at the north	(weathered granite w/ muscovite)
AA7051	γp	2X1	NNW-SSE	1		Ser predominates	
JE106	Cpa	0.5		1		central Kao with Ser fringe	(weathered granite w/ muscovite)
AA7052	CPb	2X1	NW-SE	2		Kao predominates	
AA7053	CPb	3X1.5	NNW-SSE	2			
AA7054	CPb	3.5X1.5	N-S	0.5			Quebrada de Pismanta
AA7055	CPb	2.5X1.5	WNW-ESE	1	circular structure	Kao zones are located in north and south	La Poposa
AA7056	γm	5.5X5	N-S	2	lineament (NW-SE, N-S)	Ser zones are distributed in three parts in which small Kao zones are located	
AA7057	Cpa,CPb	1.5X0.5	N-S	1		Kao predominates in central small area with small Ser zones	
AA7058	γp,CPb	3X1.5	NNW-SSE	1		Goe zones are distributed with small Kao zone	
AA7059	αm	5.5X2	N-S	1		Kao predominates in central area surrounded by Ser zones	Guanaqueros
AA7060	γp	1.5X1	NNW-SSE	1	circular structure		San Francisco de los Andes
AA7061	Psva	1.5X1	N-S	1		Kao predominates surrounded by Ser areas	
AA7062	Psva	5X1.5	ENE-WSW	1		Kao predominates in northern area and Ser predominates in southern area	
AB8001 (AA7064)	Ps,αm	6X1.5	N-S	2	circular structure	Ser and Kao distributes,Ser predominates in western half	El Retamal
AA7065	γp	2X1	N-S	2		Alu predominates with small two Kao zones surrounded by Ser zones in the north	
AA7066	αm	5X2	N-S	2	circular structure, lineament (NW-SE)	Kao predominates in western area while Ser zones are located in the east	Avestruces
AA7067	αm	3.5X1.5	N-S	2	margin of circular structure	Ser zones are located in two areas	Portezuero de Amarillo
AA7068	Trv	2.5X1.5	WNW-ESE	2	circular structure	Kao predominates in south and Ser predominates in north	Venezuera

Number of Alteration	Lithology observed	Dimension (km)	Elongation	Intensity of alteration*	Structure Texture	Alteration Mineralogy mapped by JERS-1 OPS data	Prospect included
JE107	Trv			2		Aggregate of smallish Ser alteration crots	Potrerillos
AA7069	γp	5.5X1	ENE-WSW	2	lineament (N-S, NW-SE), circular structure	Ser zone is located from west to NE with small three Kao zones in the west	Manrique
AA7070	Psva	5X1	N-S	1	lineament (N-S, E-W)	Kao predominates northern area and Ser predominates in the south	Portezuero Las Burras
AA7071	αm	1X0.5	NNE-SSW	2		Ser predominates	
AA8054	Ps	2.5X0.5	NW-SE	1	lineament (N-S, NW-SE)	Kao predominates with small Goe zone in center and small Ser zone in NE edge	
AA8070	Ps, γp,Trv	4X3	E-W	2			
AA8057	OlMiv	1X0.5	NNE			Ser predominates in the south and Kao predominates in the north with very small Alu zone	
AA8010	γp	2X1.5	N-S	2	intrusive	Kao predominates with small two Ser zones in the SE	
AA8011	γt	2X1.5	NE-SW	2	intrusive	Kao predominates with small two Ser zones in the north and south, and Goe zones are located in the edges of east and west	
AA8012	γt	2X1.5	NE-SW	2		Kao predominates with Ser zones in northern to western edge	Rincones de Araya
AA8013	γt	1X0.5	NW-SE	2		Kao predominates with small Ser zone in the southern edge	
AA8014	γt	2.5X1.5	NNW-SSE	2		Kao zone is located from NW to SE along with Ser zone	
AA8015	γt	3X2	NE-SW	1	circular structure		
AA8016	Ps	1.5X0.5	N-S	2	lineament (NNW-SSE)	Two areas divided to Ser zone and Kao zone	
AA8020	γt	3.5X2	WNW-ESE	2	lineament (NNW-SSE), intrusive	Kao predominates with Ser zone in east and south edge	El Alter, Rincon del Cenicero
AA8022	Jb	2X1.5	WNW-ESE	2		Kao predominates with Ser zone in the western edge	
AA8023	γt	2.5X1.5	NE-SW	2		Ser zone runs from NEE to WSW in which small Kao zone is located	
AA8025	Ks	6X2	ENE-WSW	2	circular structure lineament (NNW-SSE)	Kao predominates with Ser zone in SE	El Pachon
AA8028	Mii	3X1.5	NE-SW	2		Ser zones are located in the peripherals	Yunque
AA8030	Mii	2X1.5	WNW-ESE	2	circular structure	Small Kao zone in the west	
AA8049	Ks,Mipl	4X2.5	N-S	2	circular structure		El Indio
AA8058	γt	2X1	NNW-SSE	2	intrusive	Ser predominates with Kao zone in the north to west peripherals	
AA8059	γt	2X1	E-W	1	circular structure (a little vague)		
AA8060	Ps	1.5X1	NNE-SSW	1		Kao predominates with Ser zone in the peripherals	
AA8061	γt	4X1	NE-SW	2		Kao predominates with Ser and alu zones in the peripherals	
JE108	γt	1.2X0.5	E-W	1		Ser predominates	
AA8062	Olmiv	3X1	N-S	1	lineament (N-S)	Kao and Ser zones runs from S to N	
AA8066	γp,Ps	5.5X2	ENE-WSW	2			
AA8067	Trs	5X2	N-S	1			
AB7003	Cs	1.5X0.5	N-S	2	lineament (NE-SW, N-S)		Guachi, Las Tolas

Alteration

Number of Alteration	Lithology observed	Dimension (km)	Elongation	Intensity of alteration*	Structure Texture	Alteration Mineralogy mapped by JERS-1 OPS data	Prospect included
AA8056	Trv	2X1.5	NNE-SSW	2	circular structure	Ser predominates	
AA8063	Ps	1.5X1	ENE-WSW	0.5			
AA8064	Ps	1X0.5	E-W	0.5			
AA8065	Ps	4X1.5	NNW-SSE	0.5			
AA8070	Ps, γp,Trv	4X3	E-W	2	circular structure	Ser zones are scattered in three areas	
AB8003	γp	4.5X1	NNW-SSE	2			Alcaparossa
AB8004	Ps	2.5X2	E-W	1			
AB8005	Ps	2X0.5	NE-SW	0.5		Small Kao zone with Ser zone to the south	
AB8006	Ps	2X1	E-W	2			Leoncito
AB8007	SD	1X1		1			Cerro Blanco Alteration
AB8008	PR	2.5X1	NE-SW	2			La Negrita, Cortaderas, San Benicio
AB8009	S	1X0.5	NE-SW	2	circular structure		Paramillos Norte
AB8010	S	1X0.5	E-W	2	circular structure		Creston Amarillo
AB9004	C	<0.5		2	center of circular structure		Paramillos Sur

*: Point 2, hydrotherma l alteration with high confidense lavel ; pts.1, possibly hydrothermal alteration; pts 0.5, possibly mis-understanding for weathering or other clayay feature.

巻末資料 2　アルゼンティンにおける衛星画像解析結果の報告資料およびリモートセンシング・セミナーの講義資料

衛星画像解析業務に関するリモートセンシング・セミナー

1. 講　師

大 地 正 高：財団法人 国際鉱物資源開発協力協会 調査部嘱託

2. ブエノスアイレスでの講演

(1) 日時：10月9日(金), 9:00~13:30
(2) 場所：経済公共事業省・商鉱工業庁鉱業局, 鉱山博物館のセミナー室
(3) 聴講者：約30名
(4) 講演内容：平成9年度の衛星画像解析結果(LANDSAT TM画像からの変質帯抽出)および
平成10年度の衛星画像解析の中間報告(JERS-1画像からの変質鉱物組合せの推定)

3. サンフアンでのセミナー
(写真地質学的手法による画像判読技術の講義と実習指導)

(1) 日程：10月13日(火)~16日(金)の4日間
(2) 場所：SEGEMAR (Servicio Geológico Minero Argentino：アルゼンティン地質鉱山調査所)に属する地震予知研究所のセミナー室
(3) 聴講者：19名(地質鉱山調査所や大学の研究者)
(4) セミナーの内容
・13日(火) 平成9年度の衛星画像解析結果の説明 (a.m.)
平成10年度の衛星画像解析の中間報告 (p.m.)
・14日(水) 基礎的写真地質学の講義 (a.m.)
携帯用立体鏡を用いた立体視と地質判読の実習 (p.m.)
・15日(木) 応用研究の例：中国ジュンガル盆地における砂丘の分類 (a.m.)
アンデス山脈についてLANDSAT TM画像判読の実習 (p.m.)
・16日(金) 応用研究の例：カスピ海北部の汀線モニタリングと水深図の作成 (a.m.)
研修完了証書の授与式・懇親ミニパーティ (p.m.)

4. 講義資料

(1) ブエノスアイレスでの講演資料
(2) サンフアンでの講義資料
(3) 研修完了証書の見本

ブエノスアイレスでの講演資料

SATELLITE DATA ANALYSIS FOR MINERAL RESOURCES IN THE REPUBLIC OF ARGENTINA

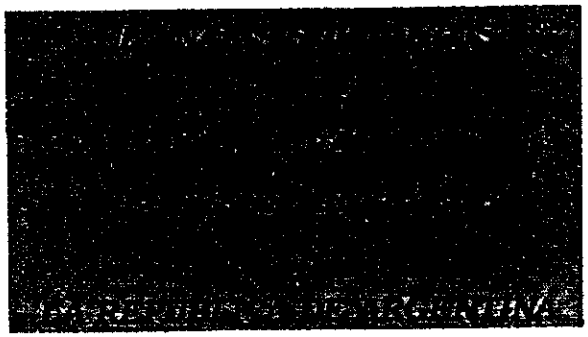

CONTENTS OF PRESENTATION

CONTENIDO DE LA PRESENTACION

PHASE-1 STUDY (LANDSAT TM)

ESTUDIO DE LA FASE 1 (LANDSAT TM)

1. INTRODUCTION
   INTRODUCCION
2. OVERVIEW
   GENERALIDADES
3. PROCESSING OF IMAGE DATA
   PROCESAMIENTO DE DATOS DE IMAGENES
4. RESULTS OF THE STUDY
   RESULTADOS DEL ESTUDIO
5. BENEFITS AND LIMITATIONS OF REMOTE SENSING DATA
   BENEFICIOS Y LIMITACIONES DE LOS DATOS DE "REMOTE SENSING"

PHASE-2 STUDY (INTERIM REPORT)

ESTUDIO DE LA FASE 2 (INFORME INTERINO)

1. INTRODUCTION
   INTRODUCCION
2. OVERVIEW
   GENERALIDADES
3. DATA PROCESSING
   PROCESAMIENTO DE DATOS
4. RESULTS OF THE ANALYSIS
   RESULTADOS DEL ANALISIS
5. ATTACHED MATERIALS WITH THE REPORT
   MATERIALES ACCESORIOS CON EL INFORME

SATELLITE DATA APPLICABLE IN GEOLOGY

DATOS DE SATELITE APLICABLE EN GEOLOGIA

SATELLITES & SENSORS (EXAMPLES)

SATELITES Y SENSORES (EJEMPLOS)

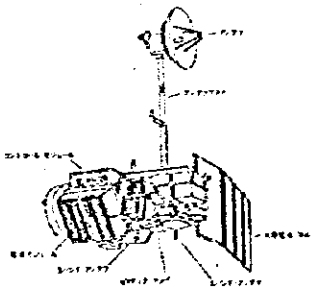

LANDSAT TM

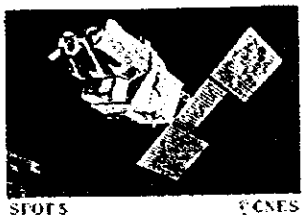

SPOT HRV

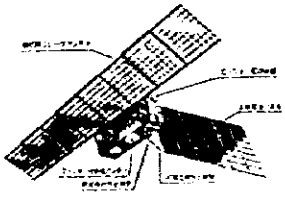

JERS-1 OVN, OPS, SAR

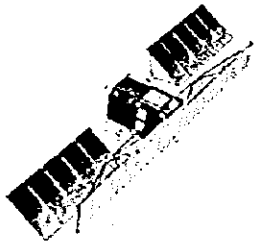

RADARSAT SAR

Spectral Coverage of Optical Sensors

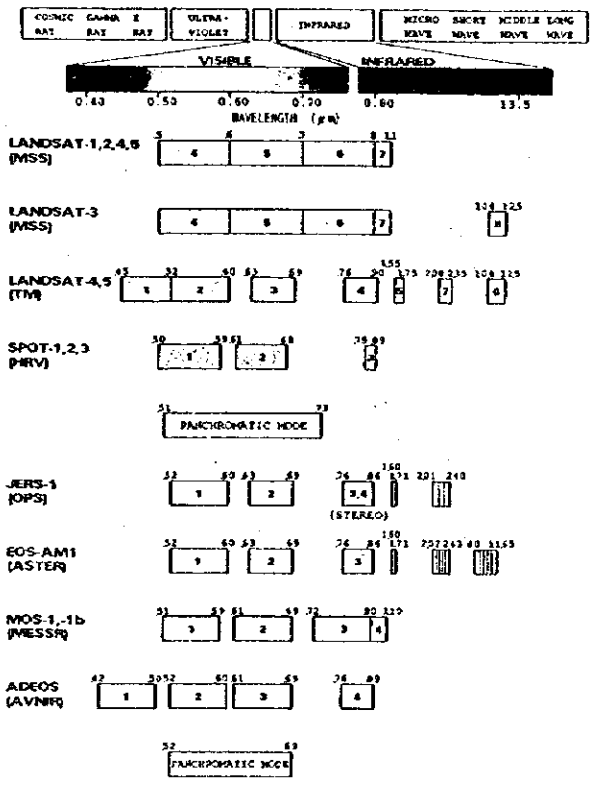

SATELLITE DATA ANALYSIS FOR MINERAL RESOURCES IN THE REPUBLIC OF ARGENTINA

EL ANALISIS DE DATOS DE SATELITE PARA RECURSOS MINERALES EN LA REPUBLICA DE ARGENTINA

CONTENTS OF PRESENTATION
CONTENIDO DE LA PRESENTACION

PHASE-1 STUDY (LANDSAT TM)
ESTUDIO DE LA FASE-1 (LANDSAT TM)

1. INTRODUCTION
INTRODUCCION
2. OVERVIEW
GENERALIDADES
3. PROCESSING OF IMAGE DATA
PROCESAMIENTO DE DATOS DE IMAGENES
4. RESULTS OF THE STUDY
RESULTADOS DEL ESTUDIO
5. BENEFITS AND LIMITATIONS OF REMOTE SENSING DATA
BENEFICIOS Y LIMITACIONES DE LOS DATOS DE "REMOTE SENSING"

PHASE-2 STUDY (INTERIM REPORT)
ESTUDIO DE LA FASE-2 (INFORME INTERINO)

1. INTRODUCTION
INTRODUCCION
2. OVERVIEW
GENERALIDADES
3. DATA PROCESSING
PROCESAMIENTO DE DATOS
4. RESULTS OF THE ANALYSIS
RESULTADOS DEL ANALISIS
5. ATTACHED MATERIALS WITH THE REPORT
MATERIALES ACCESORIOS CON EL INFORME

SATELLITE DATA APPLICABLE IN GEOLOGY
DATOS DE SATELITE APLICABLE EN GEOLOGIA

SATELLITES & SENSORS (EXAMPLES)
SATELITES Y SENSORES (EJEMPLOS)

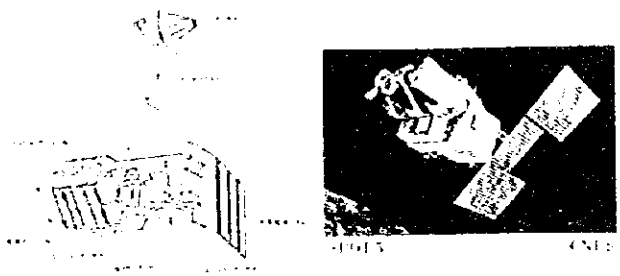

LANDSAT TM

SPOT HRV

JERS-1 OVN, OPS, SAR

RADARSAT SAR

Spectral Coverage of Optical Sensors

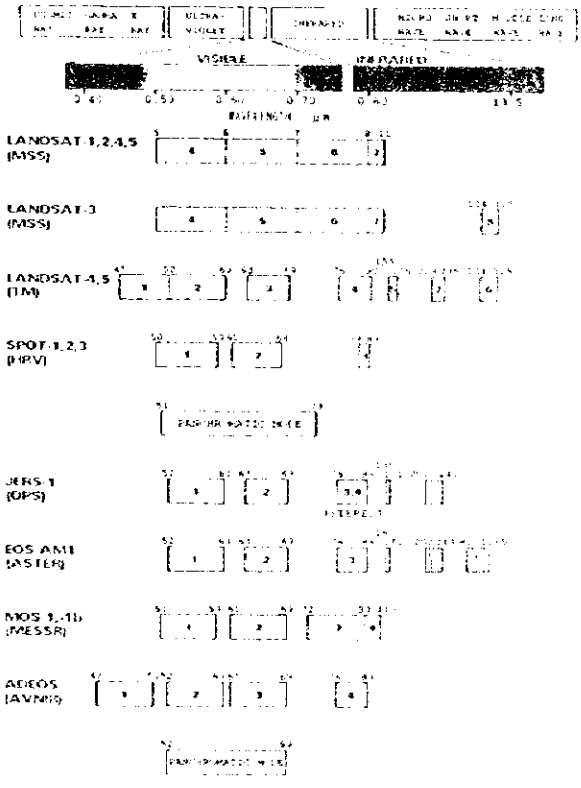

OBJECTIVE OF THE STUDY IN 1997

OBJETIVO DEL ESTUDIO EN 1997

The analysis focuses in realizing the fotogeologic interpretation using LANDSAT TM images and the results will be incorporated with published literatures for integral study of geology ore deposits and reserves on mineralization zones and will be applied for identification of zones of high mineral potential.

El análisis contempla realisar la interpretación fotogeológica mediante los imágenes LANDSAT TM, cuyos resultados serán cotejados con otras literaturas disponibles para estudiar integralmente la geología, yacimientos y reservas de las áreas mineralizadas, y de esta manera identificar las áreas con alto potencial de desarrollo.

STUDY CONTENTS IN 1997

CONTENIDO DEL ESTUDIO EN 1997

1. COMPILATION OF PUBLISHED MATERIALS
   COMPILACION DE LOS MATERIALES PUBLICADOS
2. PROCESSING OF LANDSAT DATA
   PROCESAMIENTO DE LOS DATOS DE LANDSAT
3. PHOTOGEOLOGIC INTERPRETATION OF LANDSAT TM IMAGES
   INTERPRETACION FOTOGEOLOGICA DE LOS IMAGENES LANDSAT TM
4. INTEGRAL INTERPRETATION
   INTERPRETACION INTEGRAL
5. REPORTING
   PREPARACION DEL INFORME

METHODOLOGY OF THE ANALYSIS
(PROCEDURE OF PHOTOGEOLOGIC INTERPRETATION)

[redacted]

1. PREPARATION
   PREPARATIVO (obtención y orientación de los datos satelitales, recopilación y revisión de los informes geológicos y yacimientos disponibles)
2. PROCESSING AND GENERATION OF IMAGES
   PROCESAMIENTO Y GENERACION DE IMAGINES
3. PHOTOGEOLOGIC INTERPRETATION
   INTERPRETACION FOTOGEOLOGICA
4. INTEGRAL ANALYSIS
   ANALISIS INTEGRAL (preparación del mapa de analisis integral, y cotejo con los mapas geológicos existentes)
5. FIELD VERIFICATION SURVEY
   LEVANTAMIENTO EN TERRENO
6. RE-INTERPRETATION BASED ON THE SURVEY
   RE-INTERPRETACION A BASE DEL LEVANTAMIENTO

PRODUCTION OF IMAGES AND MAPS

[redacted]

A. IMAGES

[redacted]

1. FALSE COLOR COMPOSITE IMAGES
   (1:250,000: 23 scenes)
   For lithologic structural delineation
   IMAGENES COMPUESTAS DE FALSO COLOR (1:250,000: 23 escenas) Para delineación litológica y estructral
2. RATIO IMAGES
   : 3/1, 4/5, 5/7 = BGR (Blue, Green, Red)
   (1:250,000: 23 scenes)
   For extraction of alteration zones
   IMAGENES DE "RATIO" : 3/1, 4/5, 5/7 = AVR (Azul, Verde, Rojo) (1:250,000: 23 escenas) Para extracción de zonas de alteración
3. MOSAIC IMAGE (1:2,000,000)
   IMAGENES EN MOSAICO (1:2,000,000)

OBJECTIVE OF THE STUDY IN 1997

OBJETIVO DEL ESTUDIO EN 1997

The analysis focuses in realizing the fotogeologic interpretation using LANDSAT TM images and the results will be incorporated with published literatures for integral study of geology ore deposits and reserves on mineralization zones and will be applied for identification of zones of high mineral potential.

El análisis contempla realisar la interpretación fotogeológica mediante los imágenes LANDSAT TM, cuyos resultados serán cotejados con otras literaturas disponibles para estudiar integralmente la geología, yacimientos y reservas de las áreas mineralizadas, y de esta manera identificar las áreas con alto potencial de desarrollo.

STUDY CONTENTS IN 1997

CONTENIDO DEL ESTUDIO EN 1997

1. COMPILATION OF PUBLISHED MATERIALS
   COMPILACION DE LOS MATERIALES PUBLICADOS
2. PROCESSING OF LANDSAT DATA
   PROCESAMIENTO DE LOS DATOS DE LANDSAT
3. PHOTOGEOLOGIC INTERPRETATION OF LANDSAT TM IMAGES
   INTERPRETACION FOTOGEOLOGICA DE LOS IMAGENES LANDSAT TM
4. INTEGRAL INTERPRETATION
   INTERPRETACION INTEGRAL
5. REPORTING
   PREPARACION DEL INFORME

METHODOLOGY OF THE ANALYSIS (PROCEDURE OF PHOTOGEOLOGIC INTERPRETATION)

METODOLOGIA DEL ANALISIS (PROCEDIMIENTO DE LA INTERPRETACION FOTOGEOLOGICA)

1. PREPARATION
   PREPARATIVO (obtención y orientación de los datos satelitales, recopilación y revisión de los informes geológicos y yacimientos disponibles)
2. PROCESSING AND GENERATION OF IMAGES
   PROCESAMIENTO Y GENERACION DE IMAGINES
3. PHOTOGEOLOGIC INTERPRETATION
   INTERPRETACION FOTOGEOLOGICA
4. INTEGRAL ANALYSIS
   ANALISIS INTEGRAL (preparación del mapa de analisis integral, y cotejo con los mapas geológicos existentes)
5. FIELD VERIFICATION SURVEY
   LEVANTAMIENTO EN TERRENO
6. RE-INTERPRETATION BASED ON THE SURVEY
   RE-INTERPRETACION A BASE DEL LEVANTAMIENTO

PRODUCTION OF IMAGES AND MAPS

PRODUCCION DE LOS IMAGENES Y MAPAS

A. IMAGES

A. IMAGENES

1. FALSE COLOR COMPOSITE IMAGES
   (1:250,000: 23 scenes)
   For lithologic structural delineation
   IMAGENES COMPUESTAS DE FALSO COLOR (1:250,000: 23 escenas) Para delineación litológica y estructral
2. RATIO IMAGES
   : 3/1, 4/5, 5/7 = BGR (Blue, Green, Red)
   (1:250,000: 23 scenes)
   For extraction of alteration zones
   IMAGENES DE "RATIO" : 3/1, 4/5, 5/7 = AVR (Azul, Verde, Rojo) (1:250,000: 23 escenas) Para extracción de zonas de alteración
3. MOSAIC IMAGE (1:2,000,000)
   IMAGENES EN MOSAICO (1:2,000,000)

B. MAPS

B. MAPAS

1. SIMPLIFIED GEOLOGIC MAP
   (A3 & A4 size; 23 areas)
   For lithologic, chronologic and structural correlation with results of photogeologic interpretation

   MAPA GEOLOGOCO SIMPLIFICADO
   (tamaño de A3 & A4; 23 areas)
   Para coorelación litológica cronológica y estructral con resultados de interpretación fotogeológica

2. PHOTOGEOLOGIC INTERPRETATION MAP
   (1:250,000; 23 areas)

   MAPA DE INTERPRETACION FOTOGEOLOGICA
   (1:250,000; 23 areas)

3. INTEGRATED INTERPRETATION MAP
   (1:250,000; 23 areas)

   MAPA INTEGRAL DE INTERPRETACION FOTO-GEOLOGICA
   (1:250,000; 23 areas)

4. COMPILED PHOTOGEOLOGIC INTERPRETATION MAP
   (1:2,000,000)

   MAPA COMPILADO DE INTERPRETACION FOTO-GEOLOGICA (1:2,000,000)

5. REGIONAL INTERPRETATION MAP (1:2,000,000)

   MAPA DE INTERPRETACION REGIONAL
   (1:2,000,000)

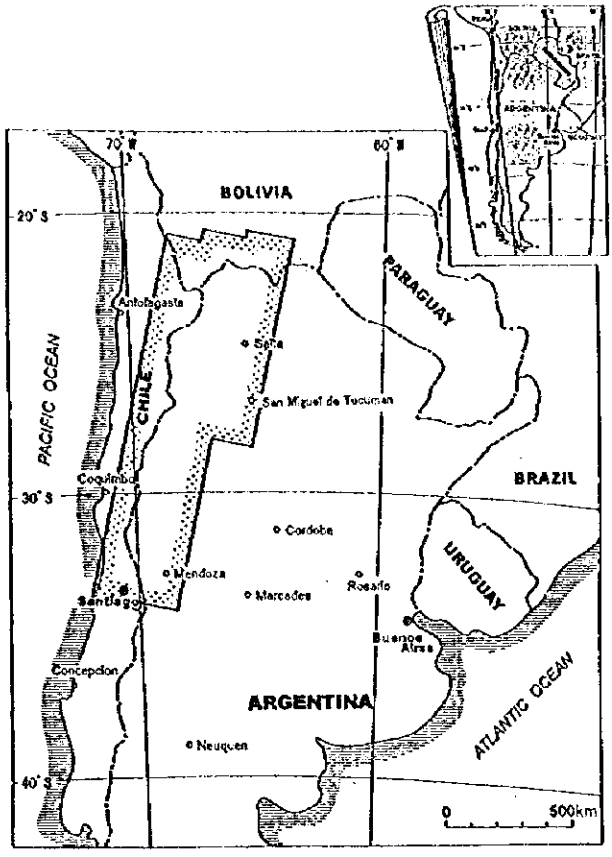

Fig. 1 Location Map of the Study Area

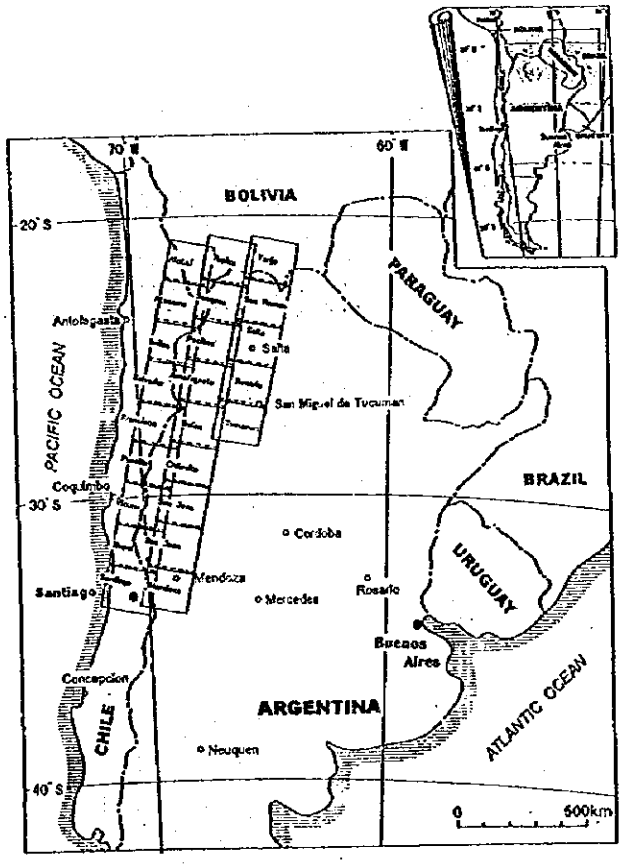

Fig. 2 Configuration of the Images Used

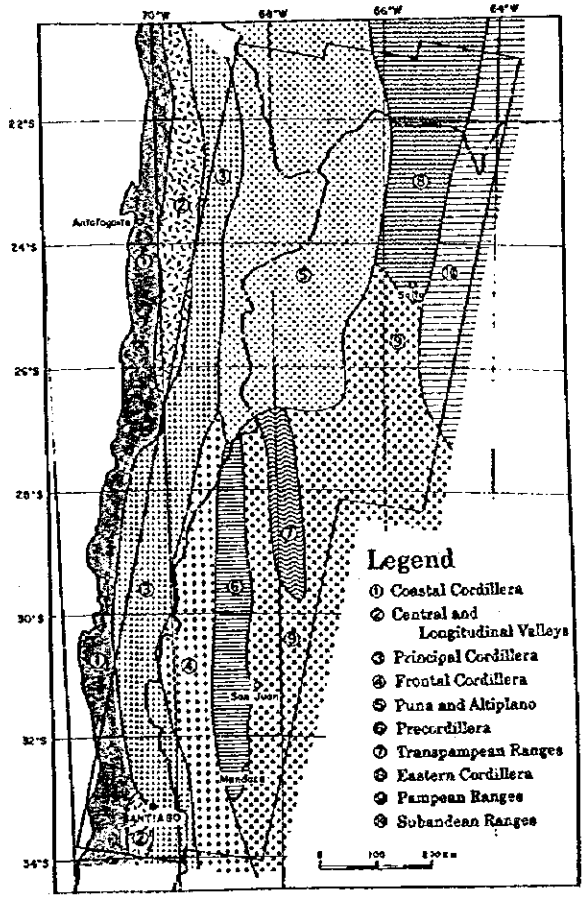

Fig. 4 Tectonic Province of the Study Area
(compiled from Sillitoe, 1981 etc.)

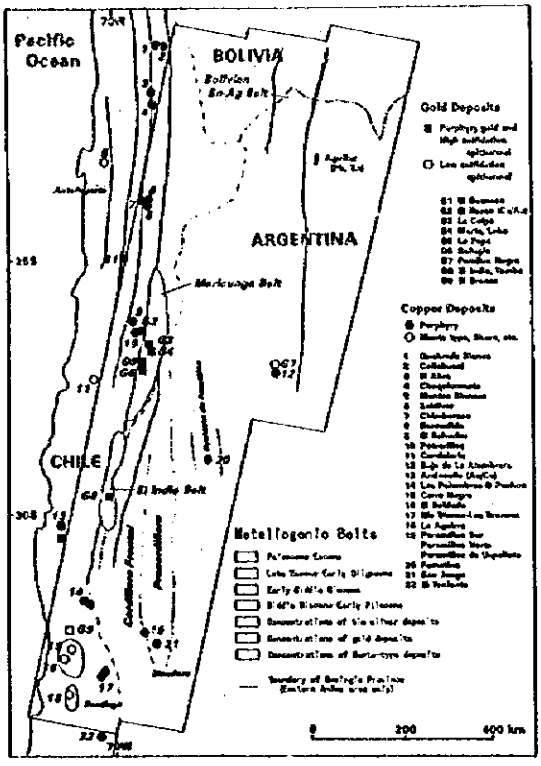

Fig. 7 Metallogenic Province of the Study Area (adapted from Sillitoe, 1991)

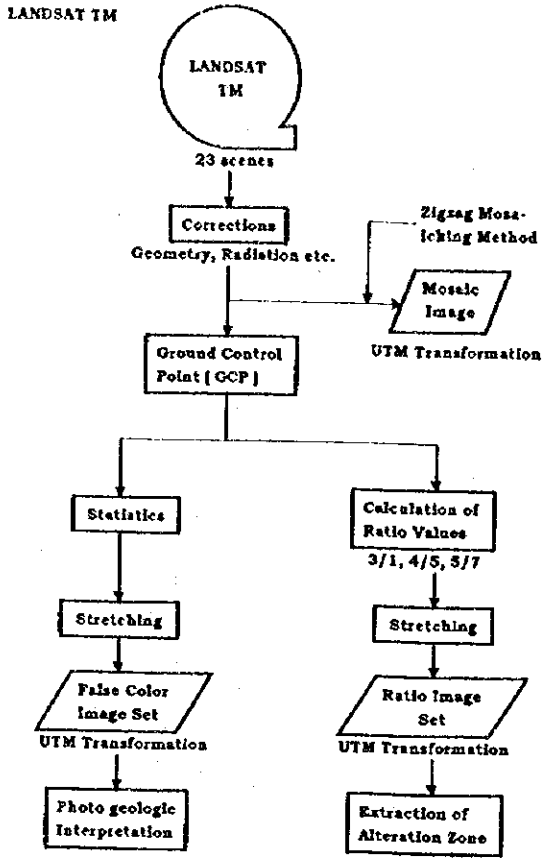

Configulation of Hardware and Software

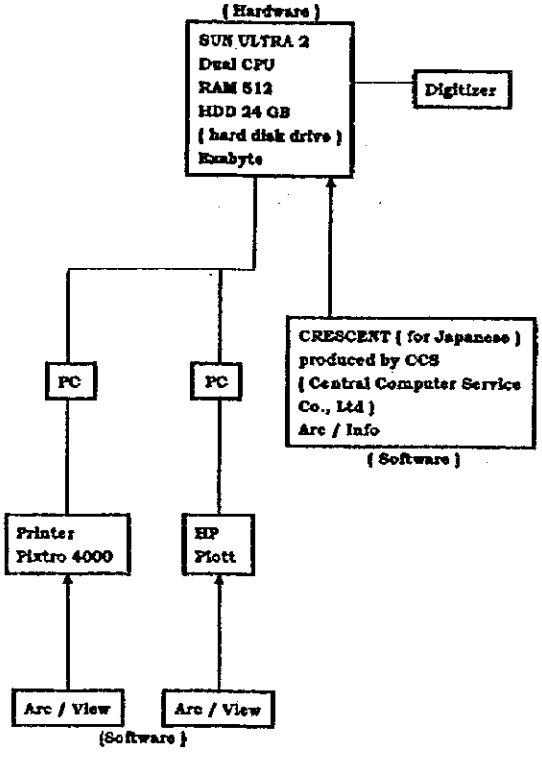

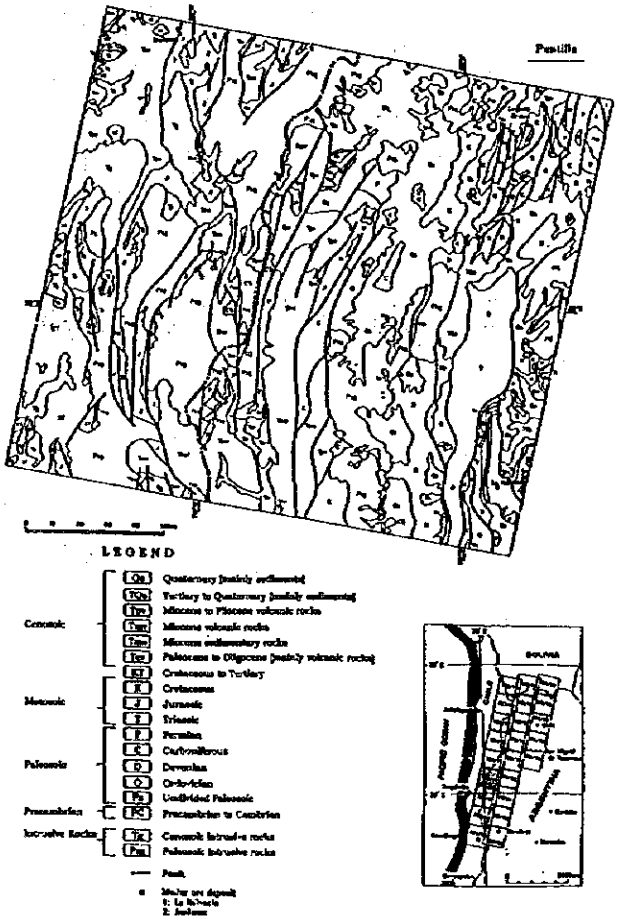

Fig.24 Simplified Geologic Map of the Puntilla Area

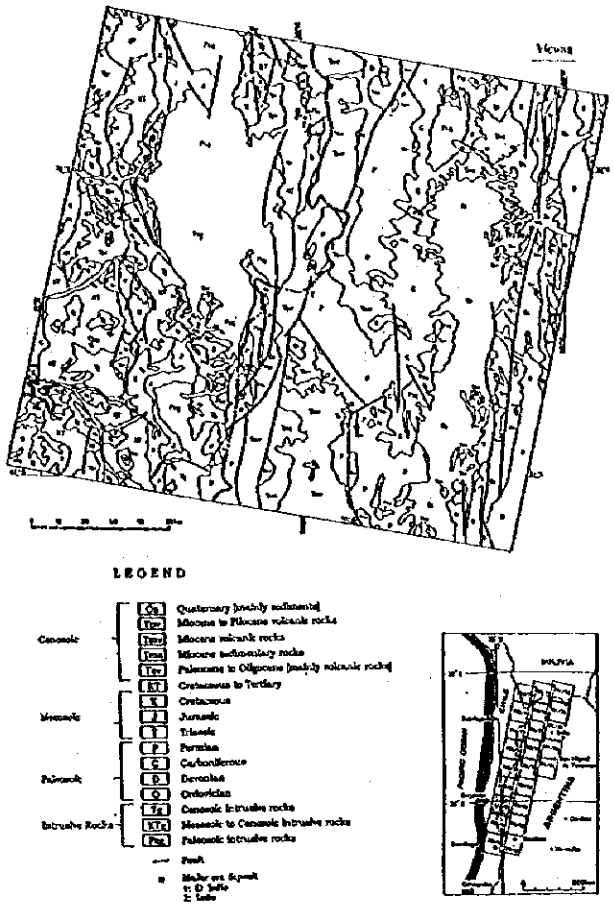

Fig.27 Simplified Geologic Map of the Vicuna Area

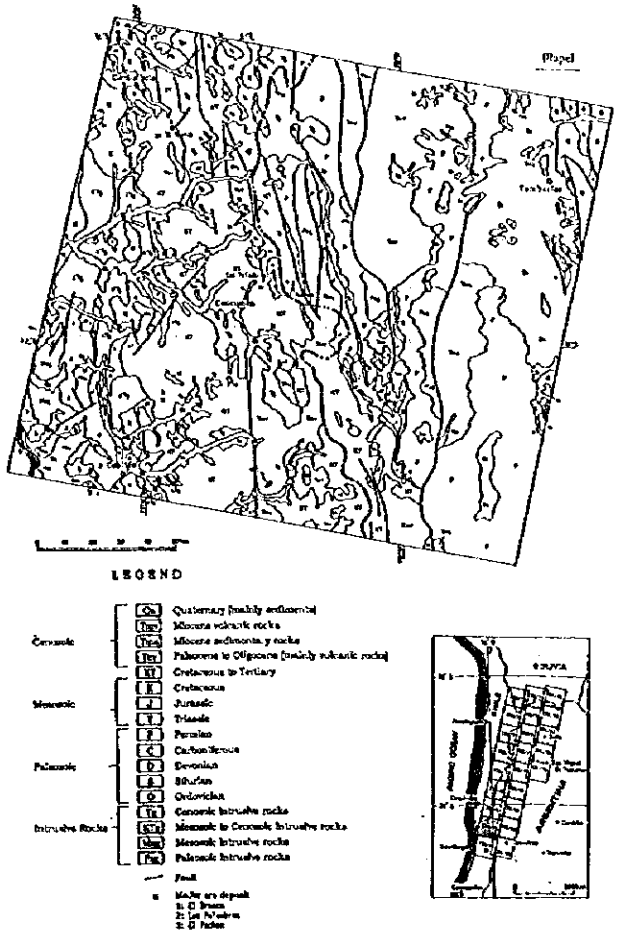

Fig.30 Simplified Geologic Map of the Illapel Area

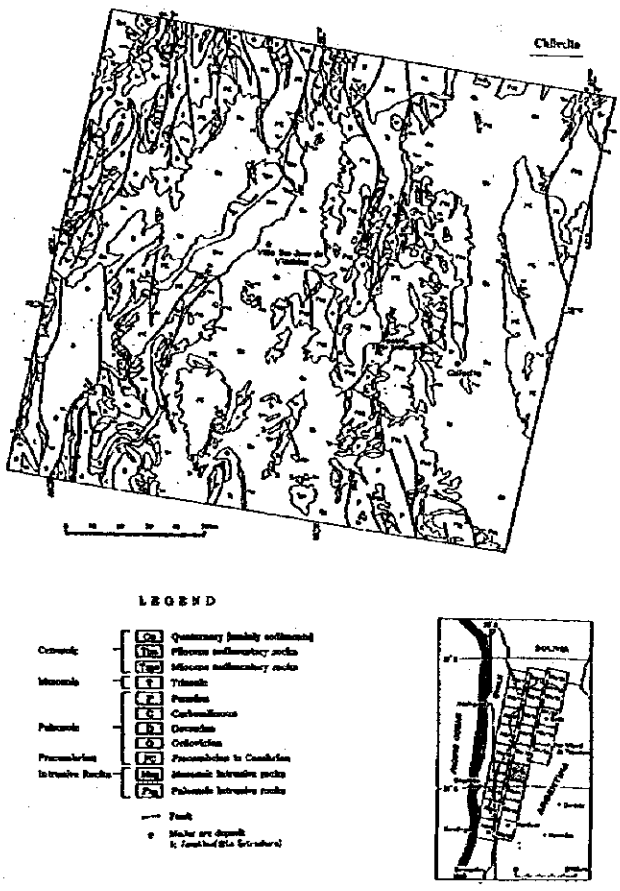

Fig.51 Simplified Geologic Map of the Chilecito Area

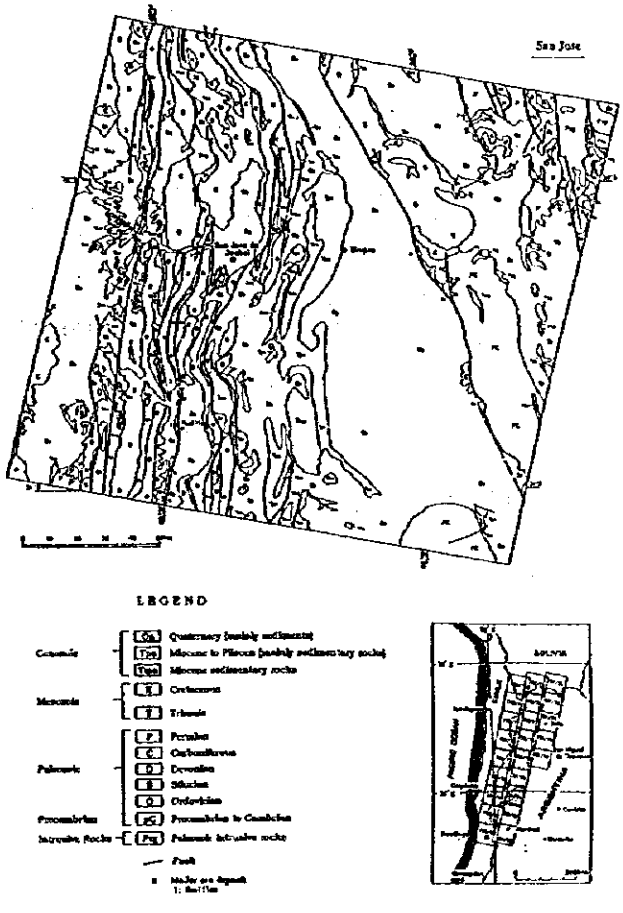

Fig.54 Simplified Geologic Map of the San Jose Area

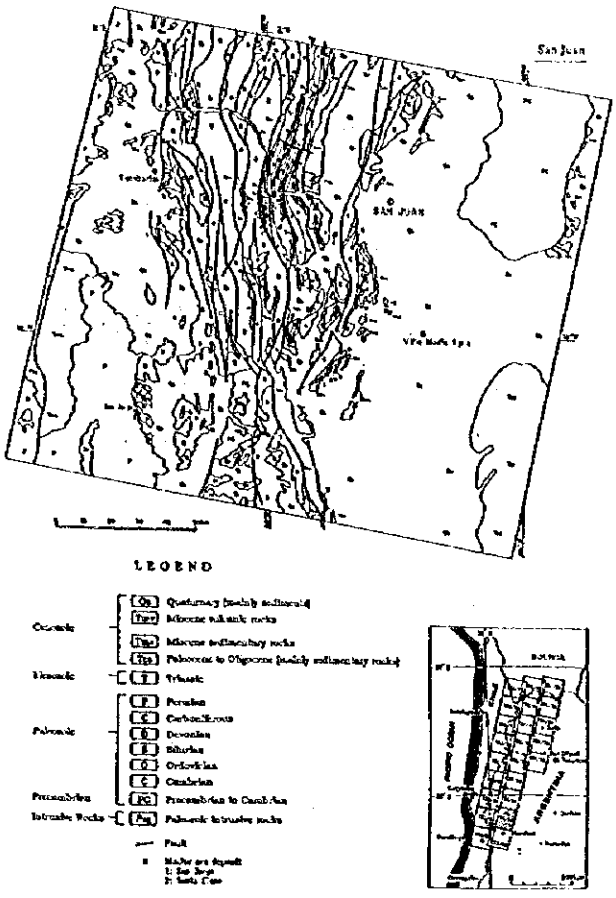

Fig.57 Simplified Geologic Map of the San Juan Area

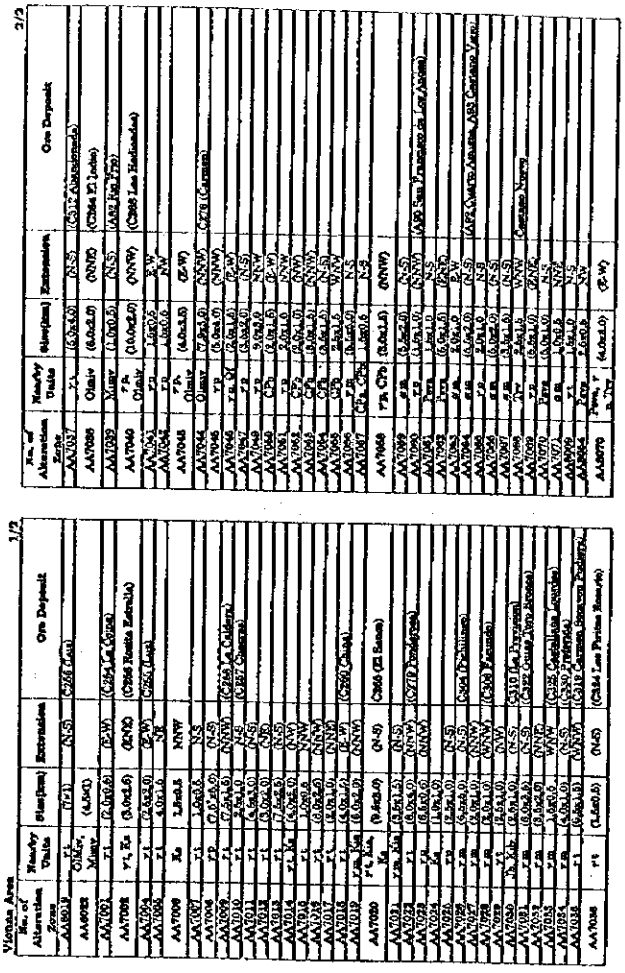

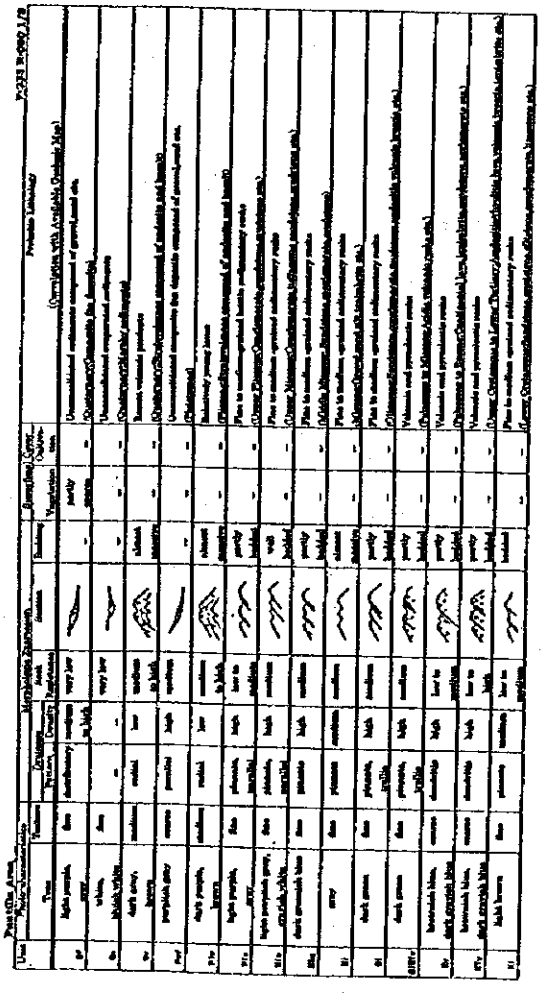

La Puntilla

Vicuna Area

No.	Name	Latitude	Longitude	Element	Type (Form)
A76	Agua Blanca and Monte Grande	29° 36'00"S	68° 09'00"W	Au, Ag, Cu	
A80	Las Aguaditas	29° 43'00"S	68° 11'00"W	Au	Vein
A81	El Salado	29° 49'00"S	69° 24'00"W	Pb, Zn, Ag	Vein (Epithermal)
A84	Rio Frio	29° 51'00"S	69° 07'00"W	Au, Ag	Vein
A88	La Puntita group	30° 00'00"S	68° 56'00"W	Au	Vein
A96	Rodolphia	30° 33'00"S	69° 30'00"W	Cu	Vein
A97	Tuvia district	30° 33'00"S	68° 34'00"W	Cu, Au	Vein
A98	San Francisco de los Andes	30° 50'00"S	68° 36'00"W	Cu, Au	Stockwork
A91	El Relamal	30° 55'00"S	68° 55'00"W	Cu, Mo	Dissemination
A92	Cuatro Amigos	30° 56'00"S	68° 57'00"W	Pb, Zn, Ag	Vein (Mesothermal)
A95	Cantaro Viejo	30° 56'00"S	69° 36'00"W	Pb, Zn, Ag	Mesothermal
A94	Cantaro Nuevo	30° 58'00"S	69° 35'00"W	Au	Vein (Mesothermal)
A96	Maria Maria Cinco and nearby mines	31° 04'00"S	69° 37'00"W	Pb, Zn, Ag	Epithermal
C854	La Colpa	29° 26'07"S	70° 07'18"W	Cu,Au,Ag	Vein
C855	Las esperanza Las Rosas	29° 07'18"S	70° 38'26"W	Au,Ag	Vein
C856	Roela Estrella	29° 29'45"S	70° 01'18"W	Cu,Au,Ag	
C857	Chacras, Chacritas	29° 21'45"S	70° 08'37"W	Cu	
C858	La Caldera	29° 52'14"S	70° 30'18"W	Cu,Ag	
C859	La China Sta. Marta	29° 30'15"S	70° 05'50"W	Cu,Ag	
C860	China	29° 58'38"S	70° 44'36"W	Cu	
C861	Juan del Valle Las Abandonadas	29° 47'44"S	70° 48'14"W	Cu,Pb,Ag	Vein
C862	Sta. Rosa Poema Esperanza Felicidad	29° 41'06"S	70° 47'48"W	Cu,Ag,Au	
C863	Flor del Valle	29° 44'43"S	70° 37'38"W	Cu	
C864	El Indio	29° 42'18"S	69° 58'17"W	Au,Cu	Bulbarmal Vein
C866	El Senon	29° 47'17"S	70° 43'06"W	Au,Ag	
C868	Aguila, Aguilucho #1-14 Diecisiete	29° 54'53"S	70° 36'39"W	Cu	Stratiform, Lenticular
C867	Delirio	29° 54'07"S	70° 50'17"W	Cu,Ag	
C868	Las Hadicndas	29° 54'52"S	70° 00'29"W	Au	Plate
C869	Bahao Victoria San Vicente Claritas Manuel A. Matta Cubana, Tula	29° 55'47"S	70° 33'12"W	Ag,Cu,Au	Stratiform, Lenticular, Plate
C870	Paraage Adriana La Beda, Escondida El Paral	29° 56'27"S	70° 30'52"W	Cu,Au,Ag	Stratiform, Plate, Manto
C871	Alto del Porongo San Antonio Manto Baja del Porongo San Juan Graciela	29° 56'45"S	70° 55'51"W	Cu,Ag,Au	Stratiform, Plate
C872	Purilama, El Volcan Sta. Ines	29° 55'17"S	70° 52'38"W	Cu	
C873	Contacto	29° 55'36"S	70° 53'41"W	Cu	Contact Metasomatic
C874	Quebrada Las Trancas	29° 58'15"S	70° 50'55"W	Cu	Vein,Manto
C875	Esperanza (Andacollito)	30° 01'11"S	70° 37'43"W	Cu	Vein,Manto
C876	Carmen	30° 02'32"S	69° 58'30"W	Au,Ag	
C877	Sta. Rosa Yuma,Socavon Quebrada	30° 02'32"S	70° 36'28"W	Cu	
C878	Esperanza	30° 04'06"S	70° 47'18"W	Ag,Pb	Vein
C879	Pundarosa (Mostaza 14) Mostaza 7 (San Pedro) San Gregorio (Mostaza 8)	30° 06'32"S	70° 41'54"W	Ag,Au,Cu	
C880	Blanca Lila La Loja	30° 06'56"S	70° 50'42"W	Cu,Mo	Stratiform, Lenticular
C881	Yuma Vieja Yuma I Santa Ana Mantos Naranjos	30° 06'45"S	70° 36'42"W	Cu	Stratiform

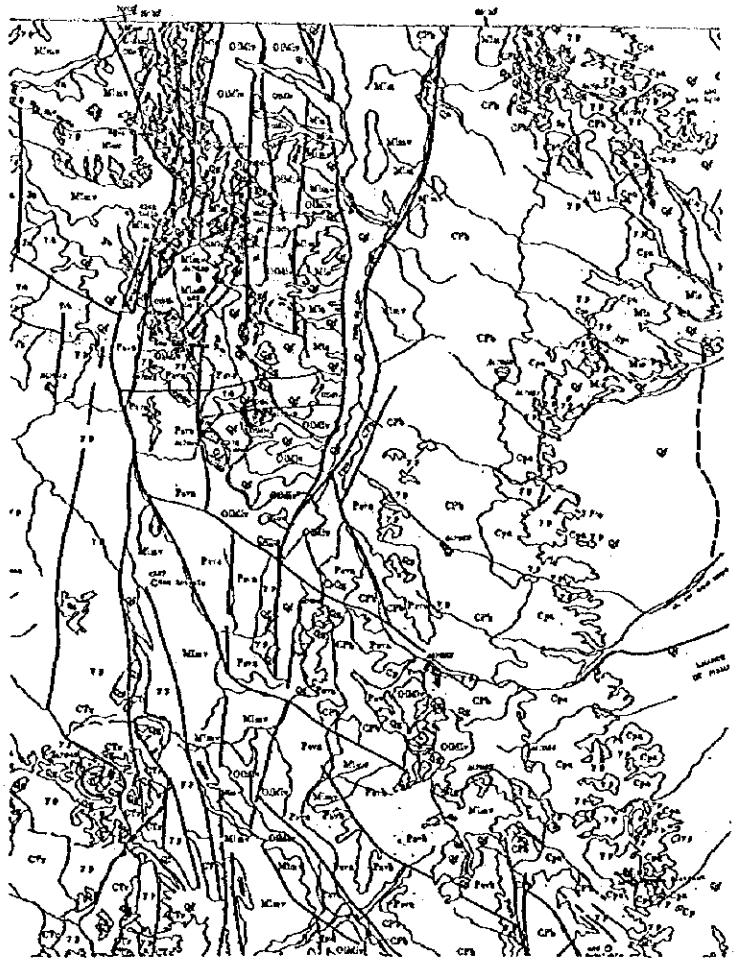

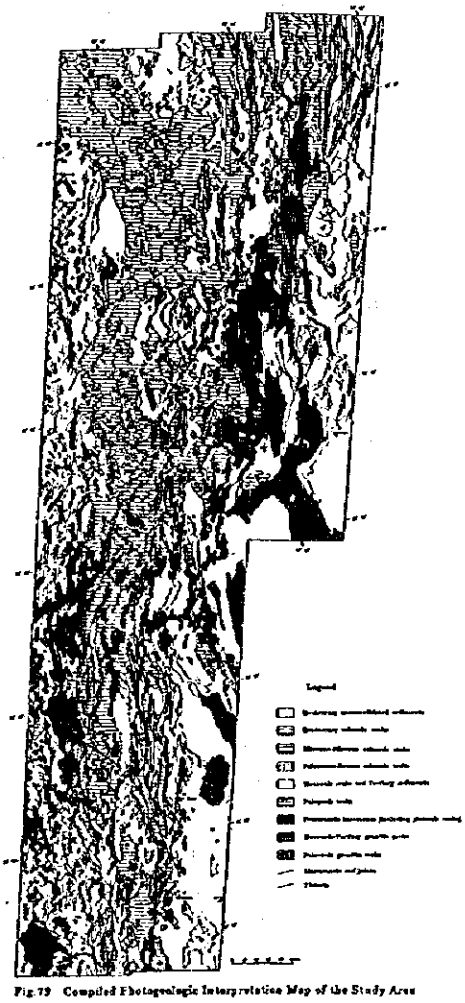

Fig.79 Compiled Photogeologic Interpretation Map of the Study Area

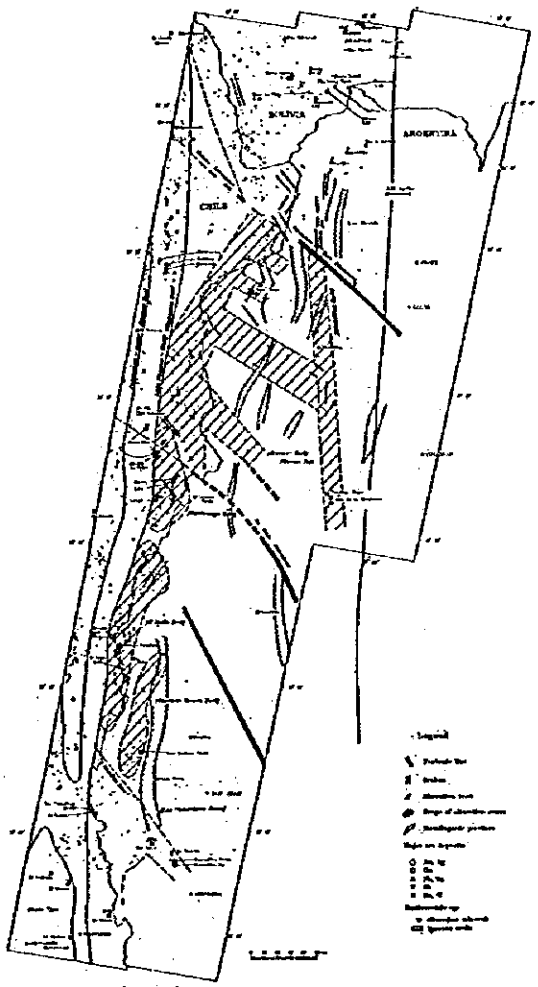

Fig.80 Regional Interpretation Map of the Study Area

BENEFITS AND LIMITATIONS OF REMOTE SENSING DATA FOR EXPLORATION PURPOSES

BENEFICIOS Y LIMITACIONES DE LOS DATOS DE "REMOTE SENSING" A FIN DE EXPLORACION

A. BENEFITS (IN REGION WITHOUT VEGETATION)

A. BENEFICIOS (EN LA REGION SIN VEGETACION)

1. MULTI-SPECTRAL DIGITAL DATA
   DATOS DIGITALES MULTI-ESPECTRAL

2. REGIONAL GEOLOGIC INTERPRETATION
   - Lithology (Photogeologic unit), Structure (Lineament, Folding) -
   INTERPRETACION GEOLOGICA REGIONAL
   - *Litología (Unidad fotogeológica), Estructura (Lineamiento, Plegamiento)* -

3. EXTRACTION OF ALTERATION ZONE
   EXTRACCION DE LAS ZONAS DE ALTERACION

4. LOGISTIC INFORMATION
   The satellite images can be utilized during a field survey as a map instead of any topographic map.
   INFORMACION LOGISTICA
   Las imagenes satelitales pueden ser utilizadas durante un levantamiento en terreno como un mapa en lugar del mapa topográfico.

B. LIMITATIONS

B. LIMITACIONES

When observing, the weather must be fine because the optical sensor cannot penetrate cloud cover.
Cuando observando, el tiempo tiene gue hacer claro porque el sensor optico no pueda penetrar la cubierta de nube.

SATELLITE DATA USED

JERS-1 OPS (VNIR & SWIR) : 9 SCENES

METHODOLOGY OF THE ANALYSIS

1. PREPARATION
2. PROCESSING AND GENERATION OF IMAGES
3. CLASSIFICATION OF ALTERATION ZONE
4. IDENTIFICATION OF ALTERATION MINERALS

PRODUCTION OF IMAGES

1. MOSAIC IMAGE
2. FALSE COLOR IMAGE
3. RATIO IMAGE
4. IMAGE OF CLASSIFICATION FOR ALTERATION ZONE
5. IMAGE OF IDENTIFICATION FOR ALTERATION MINERALS

TITLE OF THE STUDY

DETAILED SATELLITE DATA ANALYSIS FOR MINERAL RESOUCES IN THE REPUBLIC OF ARGENTINA

OBJECTIVES OF THE STUDY

The analysis focuses in detailed classification of alteration zones using Japanese JERS-1 data for the purpose of providing useful information to the field survey as well as integral study of the area.

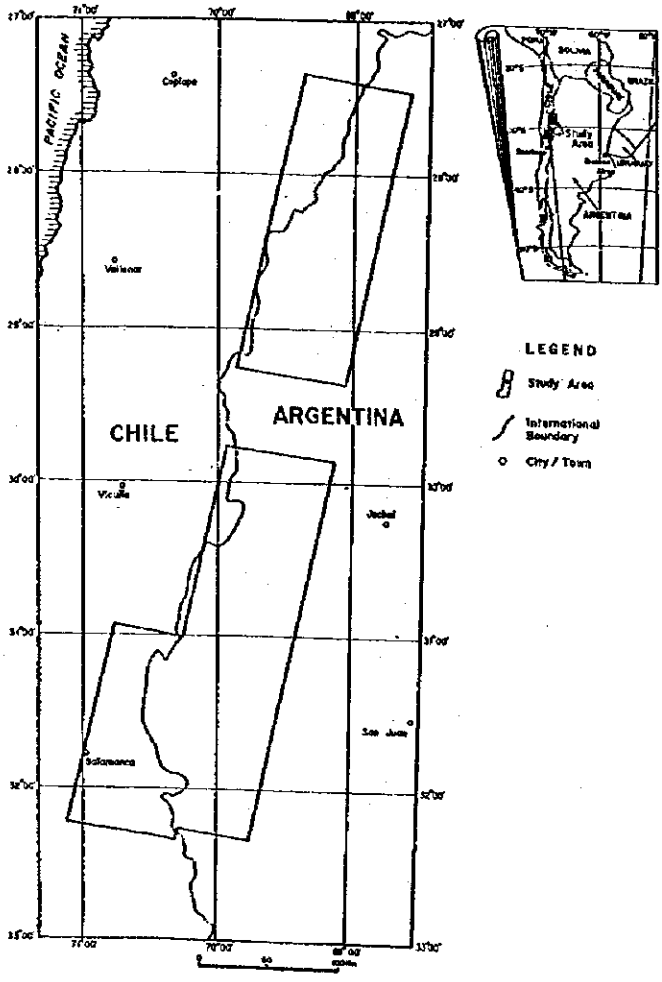

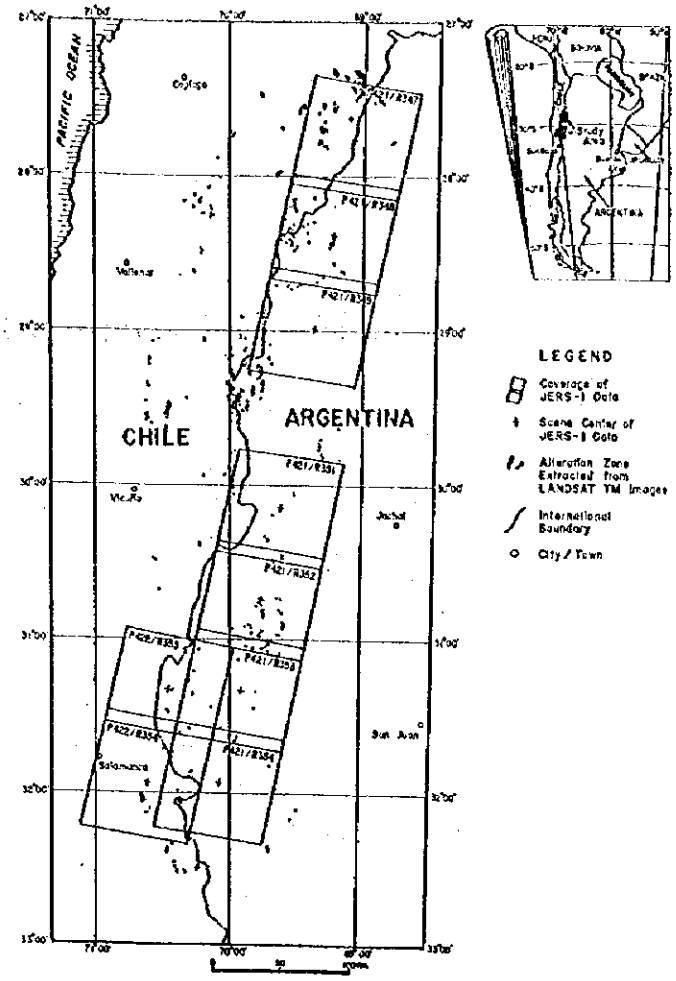

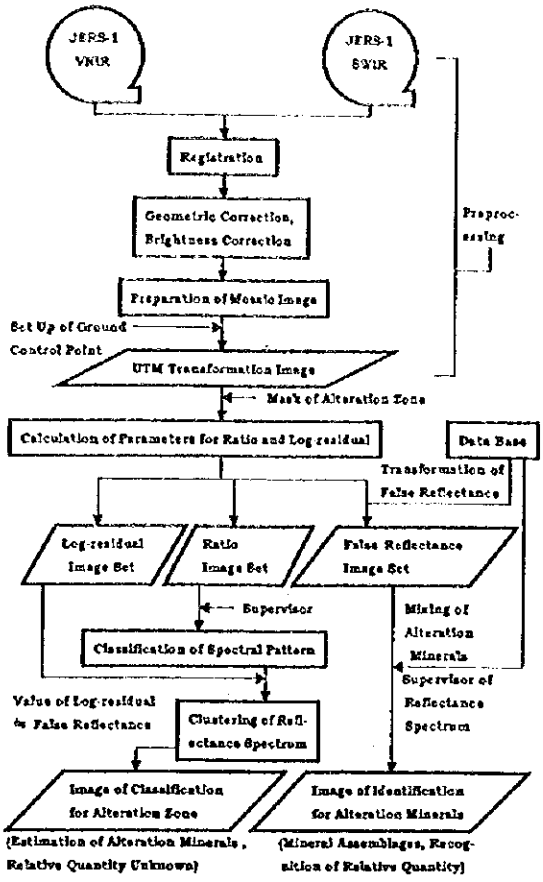

Configulation of Hardware and Software

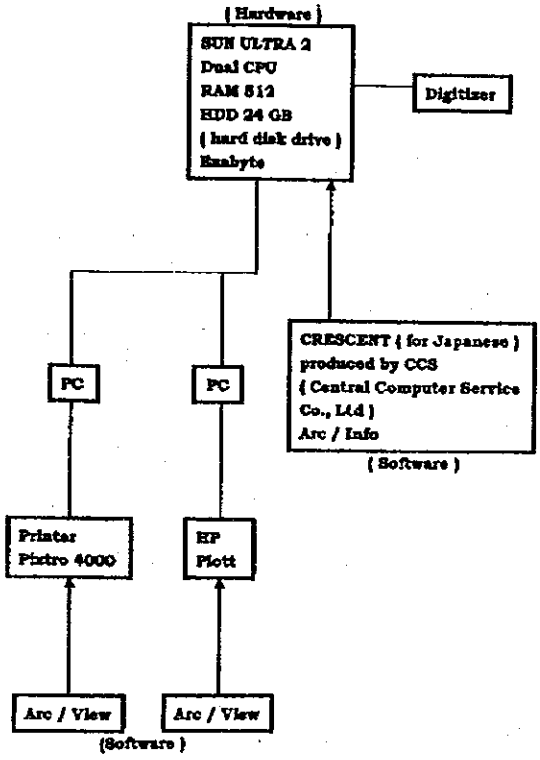

Mosaic Image

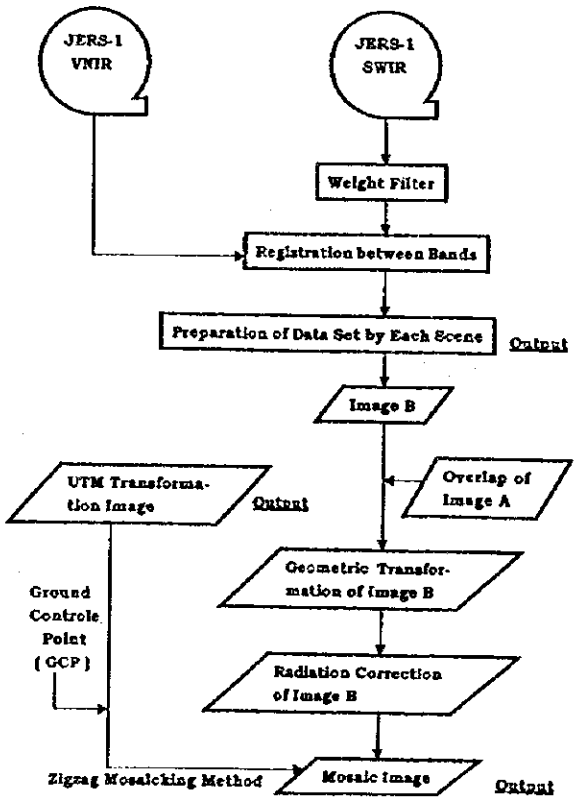

Logarithmic Residual Image and Ratio Image

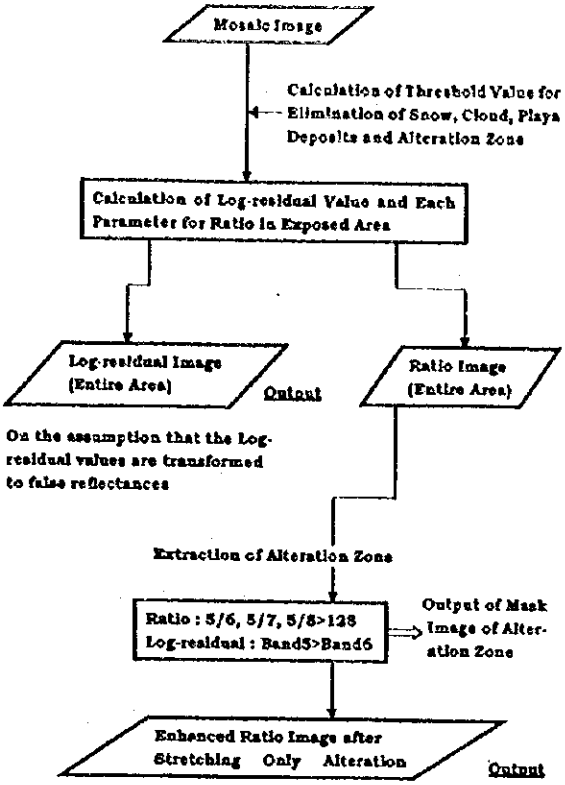

Classification of Alteration Zone

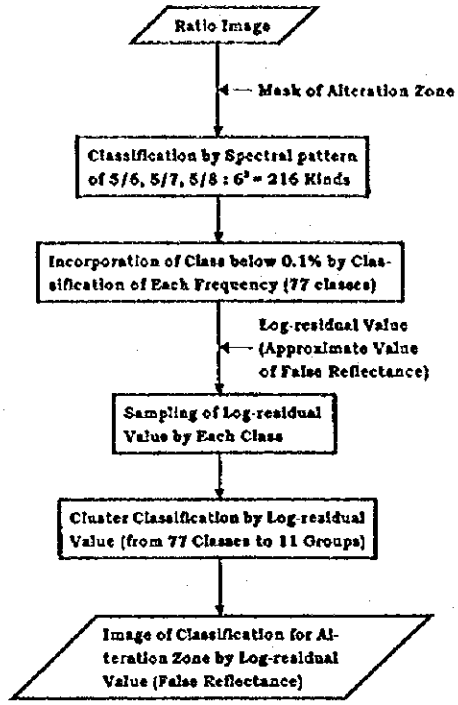

* Classification of Alteration Zone with Special Emphasis on Reflectance Spectrum *
(Rough Estimation of Mineral Assemblages, Relative Quantity Unknown)

Identification of Alteration Minerals

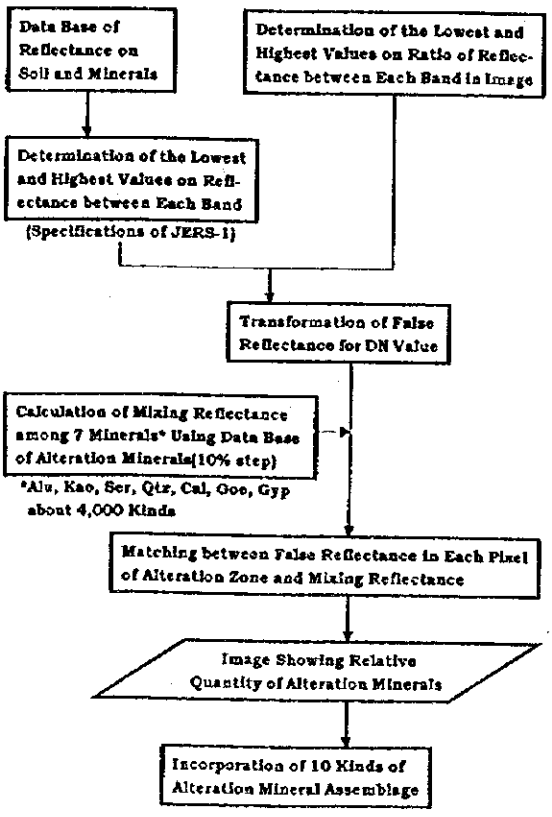

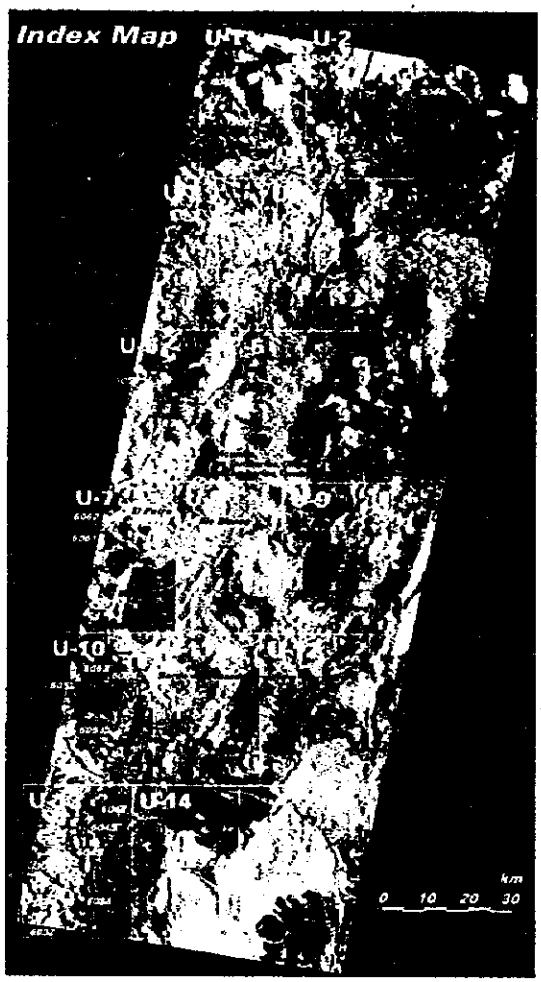

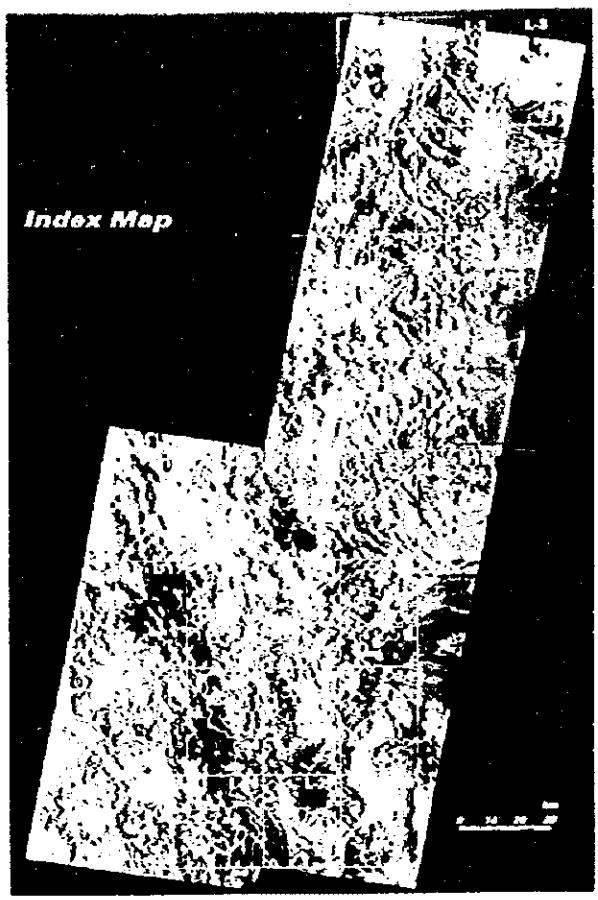

L-22 358

L-22 ratio

L-22 classification

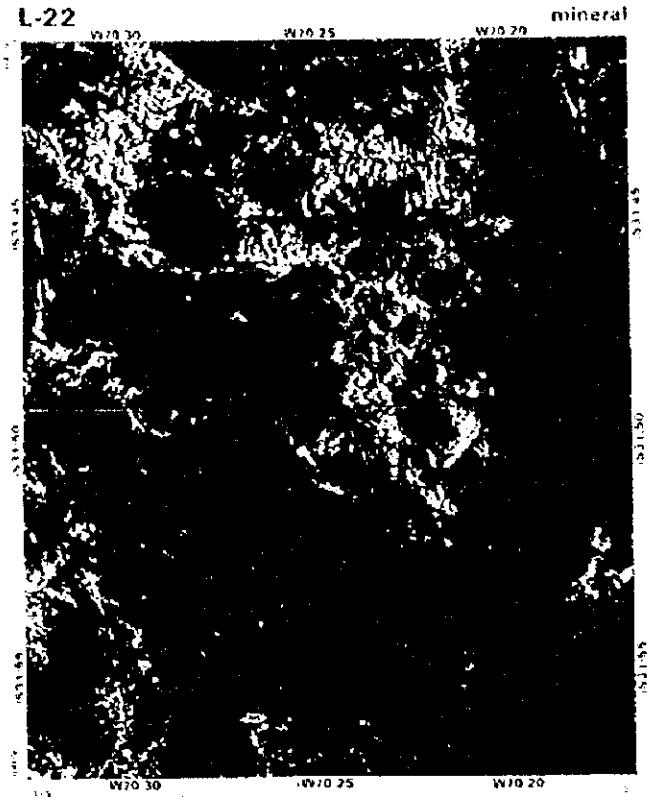

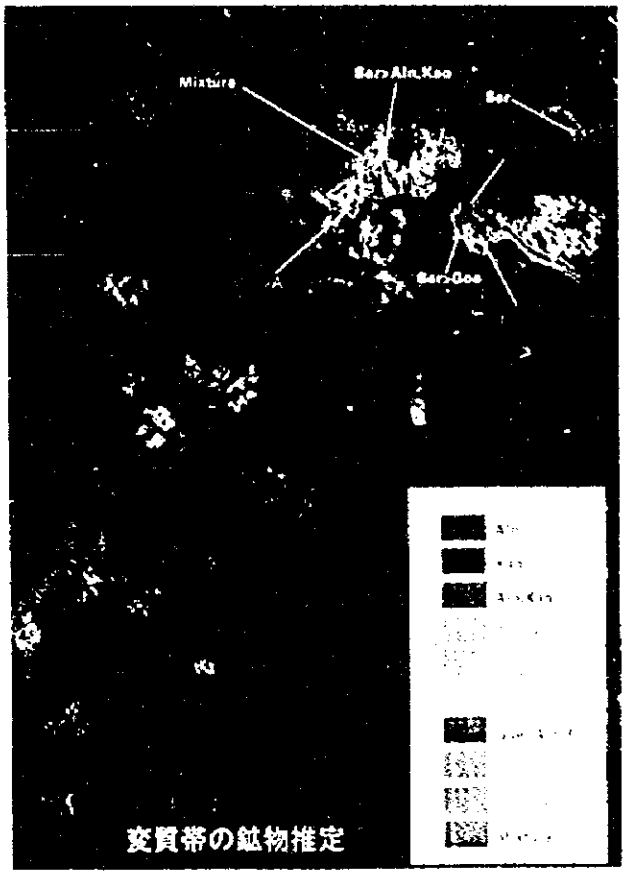

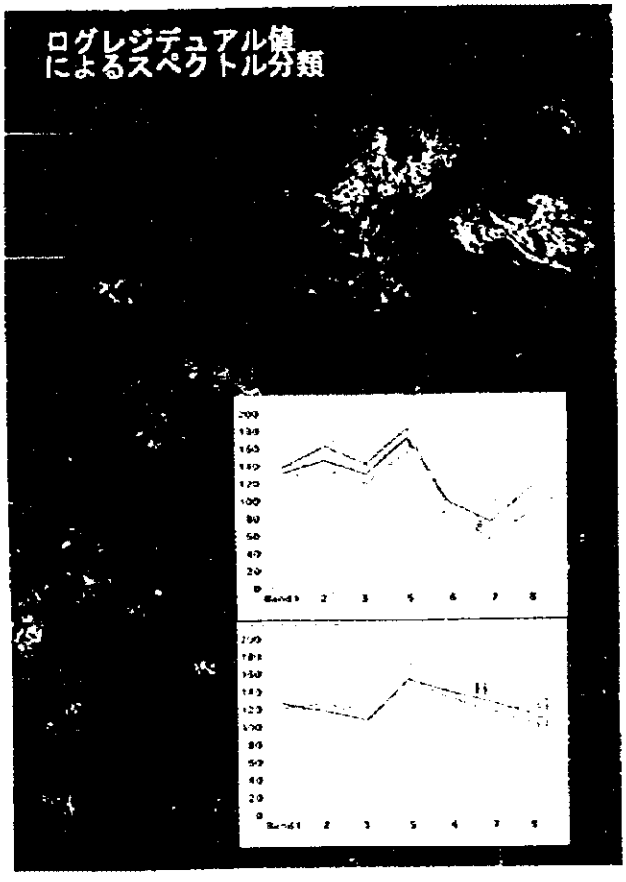

ATTACHED MATERIALS WITH THE REPORT

— IMAGES IN THE REPORT —

1. MOSAIC IMAGES (2 images in A4 size)
2. FALSE COLOR COMPOSITE IMAGE (42 AREAS: A4)
3. RATIO IMAGE (42 AREAS: A4)
4. IMAGE OF CLASSIFICATION FOR ALTERATION ZONE (42 AREAS: A4)
5. IMAGE OF IDENTIFICATION FOR ALTERATION MINERALS (42 AREAS: A4)

— APPENDIX —

LIST OF ALTERATION ZONE

— ATTACHED IMAGES AND MATERIALS —

1. MOSAIC IMAGES
2. IMAGES IN THE REPORT (9 scenes: A3 size)
3. LOG-RESIDUAL IMAGE (9 scenes: A3 size)
4. DISTRIBUTION AND CLASSIFICATION MAP OF ALTERATION ZONES

GENERAL APPLICATION OF PHOTOGEOLOGIC INTERPRETATION

— SUBJECT —

A. GENERAL GEOLOGY
1. Lithologic Mapping
2. Structural Interpretation

B. APPLIED GEOLOGY
1. Resources Exploration
   a. Metallic Minerals
      Alteration zones, Spectral analysis, Lineaments
   b. Petroleum
      Mapping, Salt dome, Folds, Lineaments
   c. Geothermal Energy
      Volcanic rock, Fractures
2. Hydrogeology
   Aquifer, Aquiclude, Structure, Basin analysis
3. Engineering Geology
   Slope stability, Landslide, Flood control,
   Prediction of inundation

C. CURRENT TECHNOLOGY
GIS: Geographical Information System
Digital Mapping Technology

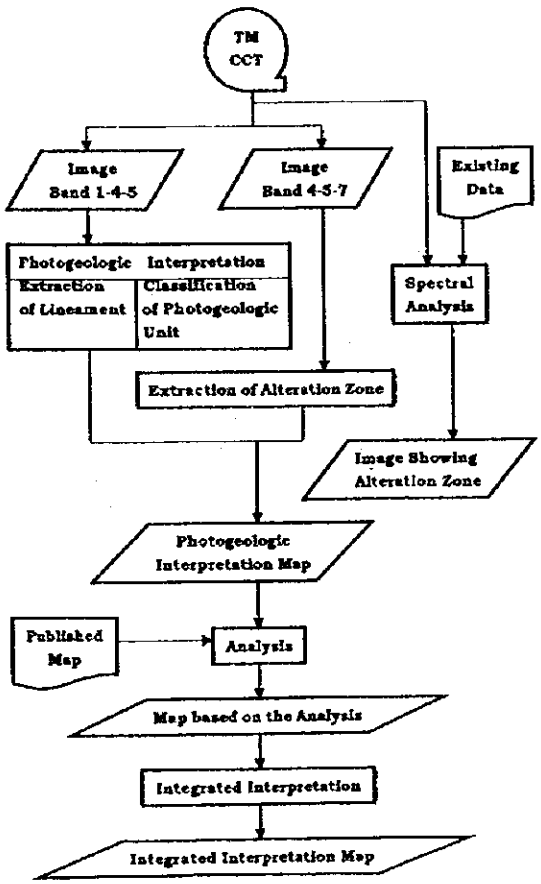

PHOTOGEOLOGY FOR MINERAL EXPLORATION

A. REMOTE SENSING DATA

LANDSAT MSS/TM, SPOT HRV,

JERS-1 OPS/SAR, RADARSAT SAR etc.

B. PHOTOGEOLOGIC ACTIVITY

1. Interpretation of Lithology
2. Interpretation of Folding
3. Extraction of Lineament
4. Extraction of Alteration Zone
5. Extraction of Logistic Information
   Roads, Urbanized Area,
   Pipeline, Railway, Airport etc.

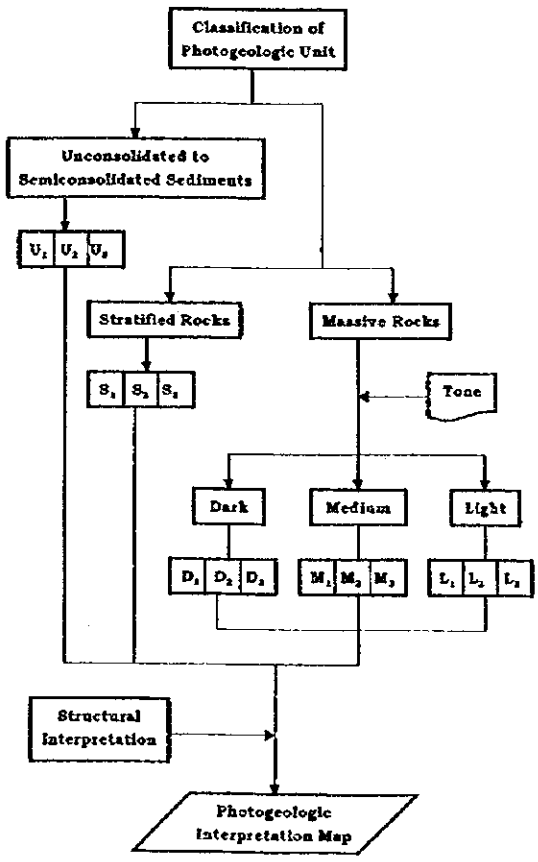

AVAILABLE INFORMATION

INFORMACION APROVECHABLE

1. LITHOLOGY
LITOLOGIA
2. FOLDING
PLAGAMIENTO
3. LINEAMENT
LINEAMIENTO
4. ALTERATION ZONE
ZONA DE ALTERACION
5. LANDSLIDE
DESLIZAMIENTO DE TIERRA
6. DENSITY OF VEGETATION
DENSIDAD DE VEGETACION
7. CULTIVATION
CULTIVACION
8. ROAD NETWORK
RANDA DE CARRETERAS / CAMINOS
9. CANAL
CANAL
10. SETTLEMENT / CITY
ESTANCIA / CIUDAD

FACTORS OF INTERPRETATION

FACTORES DE INTERPRETACION

1. TONE
TONO
2. TEXTURE
TEXTURA
3. DRAINAGE PATTERN
MODELO DE DRENAJE
4. DRAINAGE DENSITY
DENSIDAD DE DRENAJE
5. ROCK RESISTANCE AGAINST EROSION
RESISTENSIA DE ROCA
6. BEDDING
ESTRATIFICACION
7. ATTITUDE
DISPOSICION
8. JOINTING
DIACLASA
9. BOUNDARY
CONTACTO
10. SUPERFICIAL COVER; VEGETATION & CULTIVATION
CUBIERTA; VEGETACION & CULTIVACION
11. PROBABLE LITHOLOGY
LITOLOGIA PROBABLE
12. FOLDING
PLEGAMIENTO
13. FRACTURE (LINEAMENT)
FRACTURA (LINEAMIENTO)

AVAILABLE INFORMATION

INFORMACION APROVECHABLE

1. LITHOLOGY
LITOLOGIA
2. FOLDING
PLAGAMIENTO
3. LINEAMENT
LINEAMIENTO
4. ALTERATION ZONE
ZONA DE ALTERACION
5. LANDSLIDE
DESLIZAMIENTO DE TIERRA
6. DENSITY OF VEGETATION
DENSIDAD DE VEGETACION
7. CULTIVATION
CULTIVACION
8. ROAD NETWORK
RANDA DE CARRETERAS / CAMINOS
9. CANAL
CANAL
10. SETTLEMENT / CITY
ESTANCIA / CIUDAD

FACTORS OF INTERPRETATION

FACTORES DE INTERPRETACION

1. TONE
TONO
2. TEXTURE
TEXTURA
3. DRAINAGE PATTERN
MODELO DE DRENAJE
4. DRAINAGE DENSITY
DENSIDAD DE DRENAJE
5. ROCK RESISTANCE AGAINST EROSION
RESISTENSIA DE ROCA
6. BEDDING
ESTRATIFICACION
7. ATTITUDE
DISPOSICION
8. JOINTING
DIACLASA
9. BOUNDARY
CONTACTO
10. SUPERFICIAL COVER; VEGETATION & CULTIVATION
CUBIERTA; VEGETACION & CULTIVACION
11. PROBABLE LITHOLOGY
LITOLOGIA PROBABLE
12. FOLDING
PLEGAMIENTO
13. FRACTURE (LINEAMENT)
FRACTURA (LINEAMIENTO)

サンフアンでの講義資料

Texture (*Textura*)

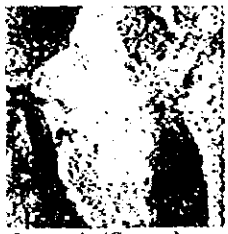

Smooth (*Suave*)

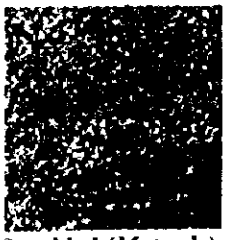

Speckled (*Moteada*)

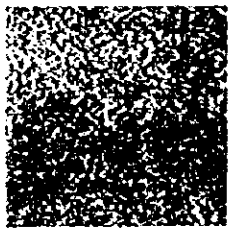

Rough (*Rugosa*)

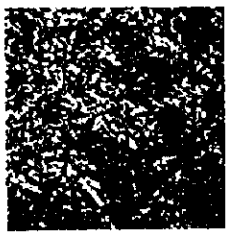

Granular (*Granular*)

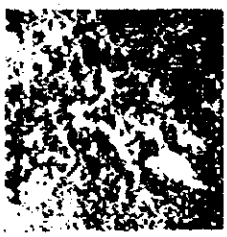

Irregular (*Irregular*)

Linear (*Lineal*)

Symbols ; Drainage (Simbolos ; Drenaje)

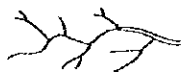

1 Stream. course visible on photographs.

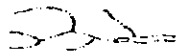

2 Intermittent stream. Dry valley

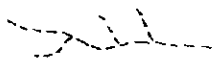

3 Stream at bottom of a valley.
Course not visible due to vegetation cover.

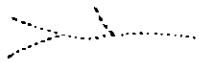

4 Approximate course of stream on lowland or terrace,
course not visible due to high vegetation.

Symbols (Simbolos)

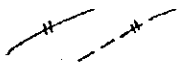

Hard bed of steep attitude, when direction of dip cannot
be observed or may be to both directions.
Frequent on hogbacks.

Strike symbols, to indicate strike of bedding plaine without
outlining shape of dipslope, with classification of dip group.

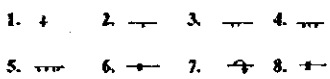

1. horizontal 2. 1/2-10 degrees 3. 10-40 degrees 4. 40-70degrees
5. 70-near vertical 6. vertical 7.overturned 8. dip direction unknown

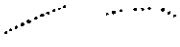

lithologic boundary, certain or supposed ;
followed on photograph.

Symbols (Simbolos)

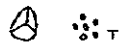

Infiltration center ; large or small in granular material,
marking kettles in glacials, small infiltration pans on terraces (T).

Hillslide, with head scarp, sliding masses and boundary

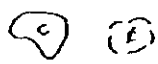

Cultivated and abandoned fields in tropical rainforest.

Alignment of vegetation.

Symbols (Simbolos)

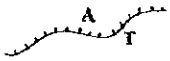

Boundary between terrace (T) and floodplain (A).

Tilt of terrace or general tilt of surface.

Hard, Resistant Beds

Ledge or rim of outcropping hard bed, which can be followed on the photographs.

Ledge of hard bed. Direction of dip can be observed, but too narrow to develop drainage or dipslope. common on escarpments.

Symbols (Simbolos)

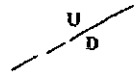

Fault with upthrown (U) and downthrown (D) side.

Downthrown side of fault direction of fault plane, dip and facet (f).

Horizontal displacement.

Small, medium and large sinkholes (with pool) in limestone, dolomite or gypsum.

Symbols (Simbolos)

Boundary of unconfomity with strike symbols.

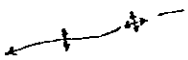

Anticline axis with dome and plunge.

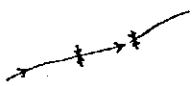

Syncline, with plunge and deepest axial part.

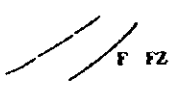

Fracture or inferred fault, F; known or certain fault.
FZ; fault or fracture zone.

Symbols (Simbolos)

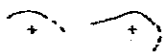

Near horizontal bedding with position of rim.

Direction of gentle dip and rim.
Arrow should be extended to foot of slope.

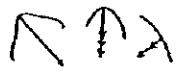

Moderate (3-10 degrees), medium (10-40 degrees) and steep (more than 40 degrees) dipslopes.
With one two three barbs.

short, narrow dipslopes, when arrows cannot be used.

Drainage Pattern (*Modelo Dranaje*)

Subparallel – Dendritic pattern (*Modelo Subparalelo- Dendritico*)

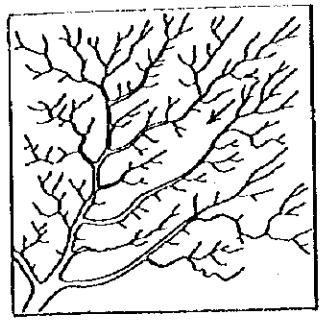

Coastal plain type . Flat bottomed broad short channels of limited extent. Elongated tributaries at the right developed due to tilt of the surface (arrow). Broad channels develop in fine sandy material.

Dendritic –Pinnate pattern (Modelo Dendritico-Pinnado)

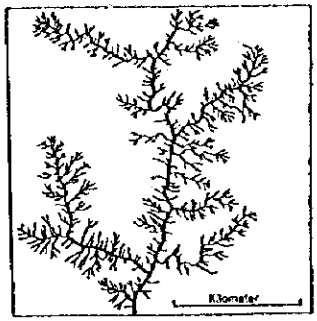

This modefication is found on Illinoan tillplain. There is no structural control. P is a plain surface. The material is sandy and clayey silt.

Dendritic-Pectinate pattern

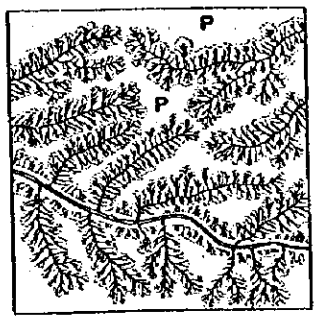

Feather-like design typical with loess. Parallel gullies with pearshaped headwater basins. Main stream in flat bottomed valley.
P is a loess surface.

Dendritic pattern (*Modelo Dendritico*)

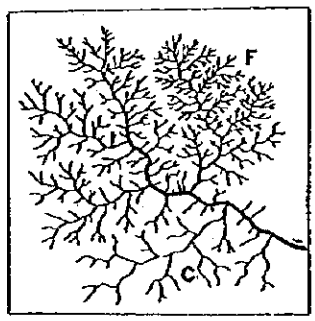

Also called tree-like or arborescent.
Most common basic pattern. F is fine texture ; C is coarse textyre.
No structural control. Occurs on fine textured impervious material.

Dendritic Pattern (*Modelo dendritico*)

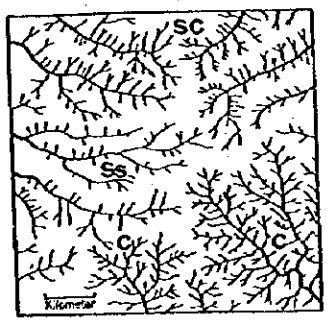

Different designs develop in clayshale (C), sandy or silty clay (SC) and sand or sandstone (Ss). The difference is in shape, ramification, type, texture and length of gullies. C is most ramified, tree-like, fine textured. S is more wide spaced, less ramified with short straight gullies. SC is foner textured with longer ramified gullies; a type between C and S.

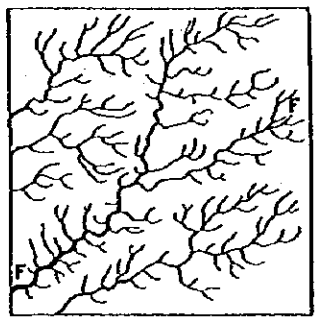

Tributaries of fourth and third order show pincer-like curved forms. Partl fracture controlled along F-F. Occurs on igneous intrusions.

Parallel pattern (*Modelo Paralelo*)

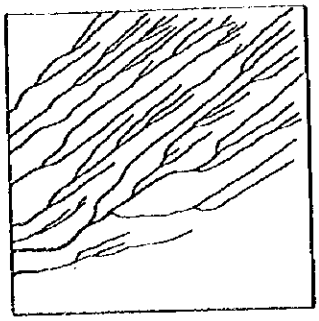

This basic pattern develops on fine textured material with steep slopes. Also along laminated formations of different resistance, e.g., sandstone-shale belts, or on tilted valley fills. It is most common along steep clay scarps with obsequent streams.

Subparallel Pattern (*Modelo Subparalelo*)

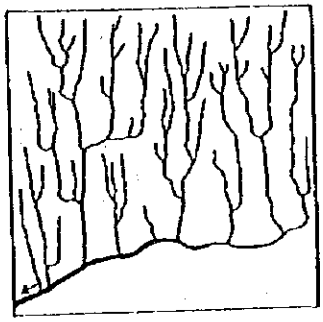

The Parallel tributaries join the main stream at an angle.this Type is common on coastal plains in fine material, or on lava streams.

Angular pattern (*Modelo Angular*)

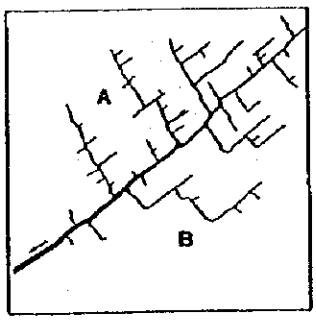

This basic type is also called a trellis pattern.
A and B are two tilted sandstone blocks. The pattern is fault controlled.
It is found on fractured grannular deposits or intrusives.

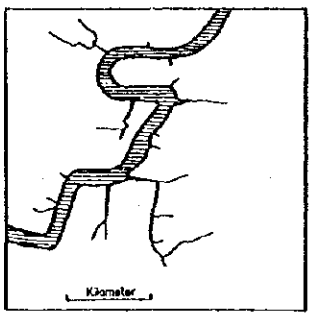

In a main stream cutting through a horizontal sandstone region. The fracture controlled channel is rounded at the top and is angular at bottom. Gully erosion develops along fractures.

Angulate pattern (*Modelo Anguloso*)

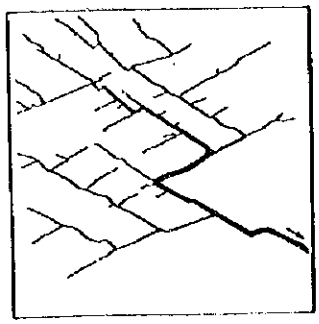

This is a modification of the angular pattern. The minor tributaries are parallel, joining the main tributaries at obtuse angles. The pattern is fracture controlled and is found mostly in granular sediments, like sandstones in near horizontal attitudes.

Contorted Pattern (*Modelo Contorsionado*)

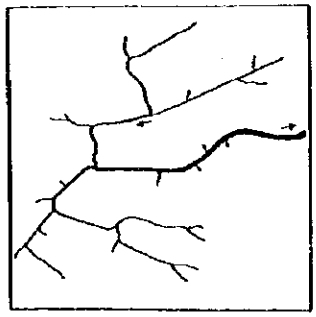

The streams show reversed flow (arrows). The material is sandstone. The control is structural.

Radial pattern (*Modelo Radial*)

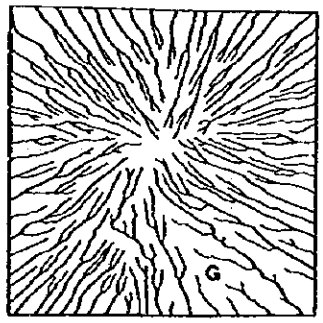

The consequent streams flow from a central area in a radial design. The design is from an Indonesian volcano. The material is fine textured tuff and granular tuff at G point. This basic pattern can be centrifugal (positive) on domes or uplifts and centripetal (negative) in basins.

Annular Pattern (*Modelo Anular*)

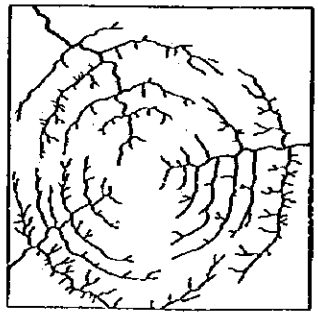

The rather rare design occurs on domes with concentric hard and soft upturned beds, or basins of similar composition.

Radial pattern (*Modelo Radial*)

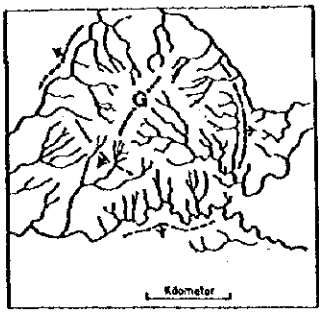

Pincerlike-dendritic and annular drainage pattern on a small granite dome. Dashed lines with arrow are hard upturned bedded sediment ridges. The central granite ridge with apex is at G point. (Meade Cy.,South Dakota)

Sinkhole Pattern

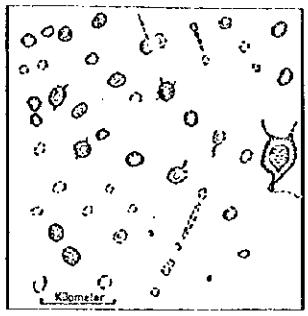

This pattern develops on soluble rocks like limestone, gypsum and dolomite. Sinks are usually roundish or oval shaped. Only short rudimentary surface channels develop. The shallow basins are filled with residual clay.

Tropical karst Pattern

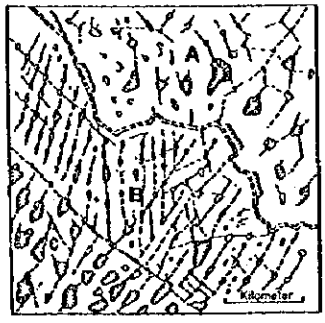

Three differen types of limestones (A,B,C) show three types of sinkholes and dissolved fractures. The dry surface channels is fracture controlled. The angular boundary between the limestone types suggest fault contact.

Deranged Pattern

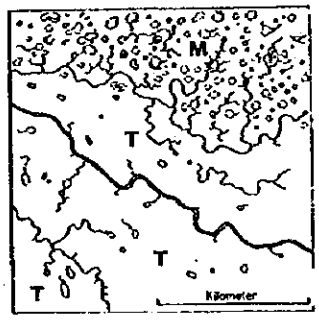

This pattern develops on gracial till. At M point is a moraine, at T points are glasial terraces. Knob and kettle topography on moraines. Infiltration centers on terraces. (New Jersey, USGS 1:20,000)

Anastomotic Pattern (Modelo Anastomosado)

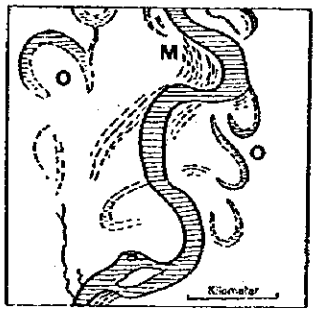

Oxbow lakes (O) and meander scars (M) are on abandoned channels. Because of the collateral commuting flood channels, the pattern is called anastomotic. This depository pattern in common on floodplains may be, in part, structure controlled.

Dichotomic Pattern

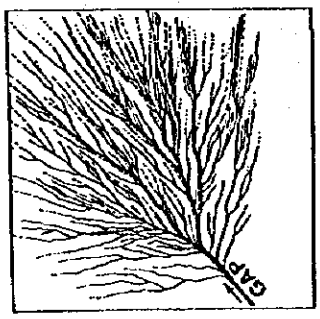

The streams radiating from a common point in a fan shaped manner depositing granular material by branching and multiple bifurcation (dichotomy). This design is found on alluvial fans and deltas.

Braided stream Pattern

This pattern develops on broad stream channels when the stream velocity becomes insuficient to carry the load of sand gravel and boulders, dumping them is the channel. This pattern is controlled by the deposited material and is very unstable. Floods may cause frequent changes.

Lacunate Pattern

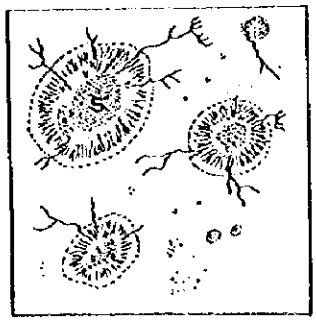

The large bowls are called buffalo wallows and occur in the Great Plains where a pervious surface layer meets an impervious substratum. Here parallel drainage develops and the water seeps into a granular deposits (S). This results in a dotted pattern (at the bottom of the bowls) of small infiltration centers, similar to those developed on terraces.

Barbed Pattern

This design occyrs on pirating streams utilizing pirated tributaries. It is also called back band drainage because the tributaries join the main stream at obtuse angle. A barbed pattern is often structurally caused.

Subdenditic Pattern (*Modelo Subdendritico*)

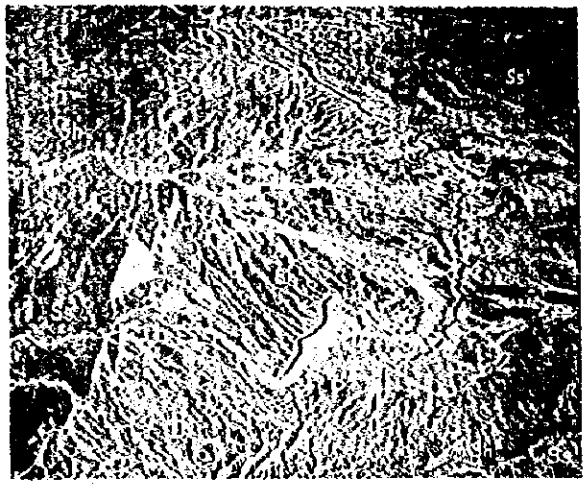

Subdendritic pattern at D^1,D^2,D^3 of three adjacement drainage basins. There are three head water basins in shale (sh^1). At left, in area 1, stream enters into sandstone zone (Ss) with coarse dendritic pattern and at shale complex (sh) with a fine textured dendritic pattern. Stream system at area 2 (right) flows in opposite direction of system 1. However, stream system 1 begins to drain system 2 at P-P along the scarp. This is stream piracy . There is a contorted stream channel at x. Ss^1 is a hard sandstone resting on Sh^2 . Double arrows indicate direction of flow. The beds are near horizontal. (Morocco)

Morphologic expression and drainage pattern of sandstone

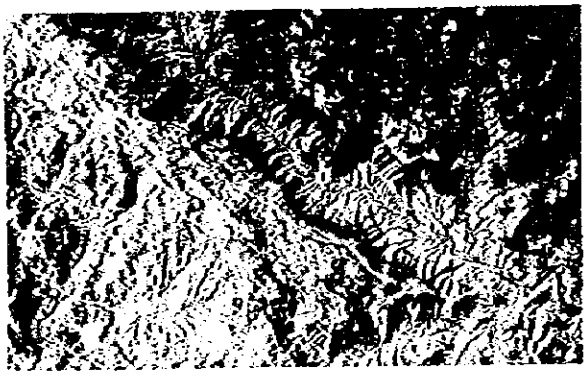

Morphologic expression and drainage pattern of sandstone (Ss) ; shale, (1,2,3) and sandy shale (X-X), in horizontal position. Separation can be made by difference in drainage pattern (dotted line). At 2 is a dendritic centripetal drainage basin ; at 3 subparallel design which develops mostly on steep finer grained clayey slopes. Note fracture controlled dry channel at F. (northern Lybia)

Dendritic pattern in fine textured shale

Dendritic pattern in fine textured shale at D.
On sandsheet (sd) only faint traces of a pattern are visible. Sandstone complex (Ss) form bogbacks with internal drainage. Desert climate, no vegetation. (Mauretania)

Centrifugal radial drainage pattern on pyroclastics (R) and parallel pattern (P) on lava streams. Volcanic region in arid climate.

B is black basalt. Granular pyroclastics around crater C have a lighter tone. (Western Sudan, Central Sahara)

Angulate and angular drainage pattern in a sandstone shale area

The type is angulate at A and near rectangular at R. The sandstone is partly thick and massive at M, but rather thin bedded at X ; here it is folded and peneplained. Drainage develops along fractures of the leveled sandstone structures. The fracture pattern is accentuated by vegetation along the crush zone. At V is a valley in a soft rock with an angulate-dendritic pattern. (Northwest, Australia)

Drainage density

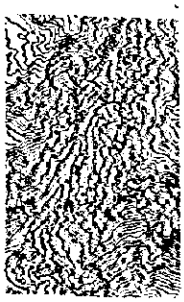

High

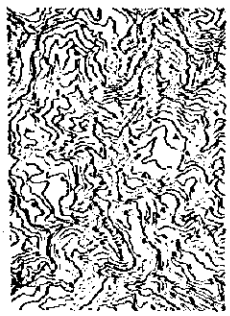

Moderate

Low

Relation of attitude of resistant beds to landform

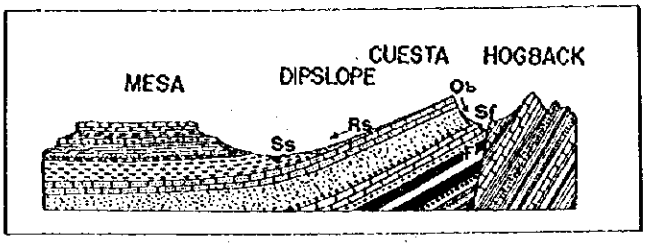

Hard beds from a mesa when horizontal, a dipslope or cuesta when tilted, and a hogback when in steep attitude. Ss is a strato subsequent or strike controlled stream ; Sf a fault controlled stream ; Rs a resequent stream, and Ob an obsequent stream. F is a fault contact between beds of moderate dip and steep attitude.

Horizontal shale formation capped by sandstone

The resistant hard sandstone forms steep cliffs. The weak crimbles into coalescent talus cones, which form a continuous sheet.
Cliff and slopes in a canyon indicate hard (sandstone, limestone) and soft (shale clay. silt) beds if the attitude is near horizontal. The light bottom of the valley is filled out by loose sand. Shale and sandstone are colored. At X is a resistant homogeneous mass, probably an igneous. (Palestine)

Bedding (Estratificacion)

Relation between strike-dip-bedding plane and talus

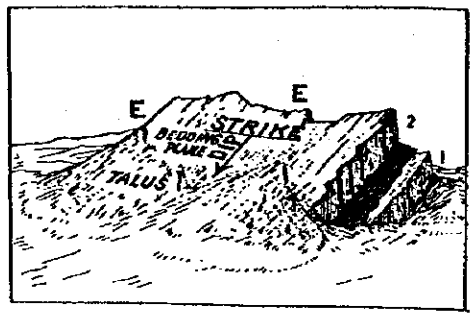

The talus tends to reduce the angle of sloping. E-E is the edge or rim of a hard bed, usually marked on aerial photographs and maps.
Number 1 is the older, number 2 the younger sandstone bed, interbedded with dark schist. Direction of strike and dip in the field is measured by a compass. The degree of the dip by clinometer. On aerial photographs steroscopic instruments are used.

Continuity analysis of an oriented mosaic sheet section

Lithologic units A-H can be followed, mainly by drainage pattern. The boundaries can be plotted without stereoscopy, which has to follow later. Unit E (a sandstone-shale complex) with boundaries to G and D is a conspicuous key horizon tree-like drainage which can be followed here over a distance of 19 km. The structure is a pitching syncline. Position of the axis is conjectural. The direction of the dipping beds can be derived from the guirlanding and V form of dipslopes, and the runoff directed towards the center of the bowl. Indications of fracturing are truncations (Tr) discontinuity of keybed with straight stream channel at X-X-X ; angular stream bends at X' and stream along straight boundary between H and G.
Facial change at top of G grading into more shaley H. (Mosaic, Utah)

Thin sandstone beds disclose structural features

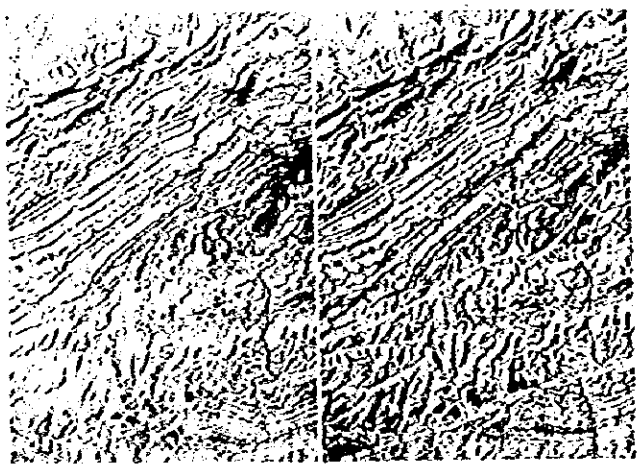

The formation is composed of rather thin, shale-interbedded sandstones. The flaggy sandstone beds can be easily followed and separated because of their individual character. The *garland pattern* is caused by thin shale intercalations on beds with medium (10-15 degrees) dip. S is a hard sandstone complex; S1 is a flaggy complex with thicker shale; S2 has thinner shale intercalations; S3 is a thick sandstone bed. The shaley anticline core, marked by axial symbol, has a duplicated sandy shale flank (note drainage pattern at sSh) of different character than flank S-S3 because of three parallel faults of considerable throw. At X-X are shale formations, eroded to valleys. At A, axial displacement. (Southern Sahel, Tunisia)

Attitude (disposicion)

Bowl shaped synclinal valley

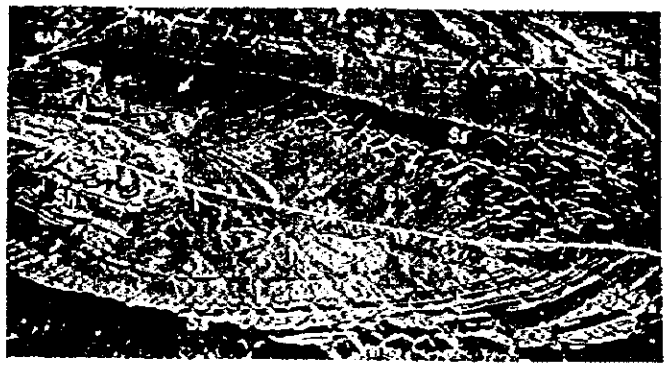

This pratically undisturbed structure is in contrast to the displaced hogback series (H) in the background. Consequently, the area H must be older, because it has its separate fault tectonics. The hogbacks have steep beds with attitudes. The synclinal bowl in the foreground has gentle undisturbed dipslopes. This indicates an unconformity between the two morphologic units. The bowl, an outstanding example of a syncline, is composed by sandstones (Ss) and shales (Sh) which are more exposed to denudation. The consequent radial drainage towards the syncline axis discharges through the watergap at the upper left corner. The oblique photograph taken at an angle of about 30 degrees does not show the dips at the foreground well, unless the dip is under the tilt of the camera. (Bou Anane, Northern Sahara)

Dislocated anticline nose

The axial displacement happens along the principal fault F-F. The upper block is sunken because Ss2 does not reappear in the center of the upper block. The left flank is steep, right flank gentle. photographic supposition like this has to be field controlled, to investigate identify of sandstone horizons (abc). At X inclination of small dipslope will indicate axial pitch. (Wyoming)

Plunge of an assymetric anticline

The beds are not disturbed by major faulting. The light toned key sandstone beds are Ss1 and Ss2. The lower flank is somewhat steepwer than the upper of Ss2. This causes assymetry. At the bottom are near vertical sandstone beds forming hogbacks (Hb). Note change of strike in steep beds along F. At T is a terrace with spotty vegetation, often found on terraces. (Hot Springs, Wyoming)

Boundary (Contact)

Following beds and plotting boundaries of hard beds, drainage pattern and tonality in an arid climate

The 13 lithologic units are arbitary chosen. Most outstanding and to be chosen for a keybed is 6. It is a very light-toned calcareous shale, wedging out at Y. Note the small close spaced gullies at right center. 1,5,9,13 are sandstones indicated by scarps. Darkest is 5 (red brown sandstones with thin sandy shales). At 3 is alluvium. Arrows indicate direction of dip. At X, dark sandstone 5 is down-thrown. Bed 11 has two sandstones S_1 and S_2 ; S_1 wedges out. Identity of chosen units, formation contacts and fault indications should be field controlled. (Big Horn Mountains, Wyoming)

Jointing (Diaclasa)

Limestone of different composition

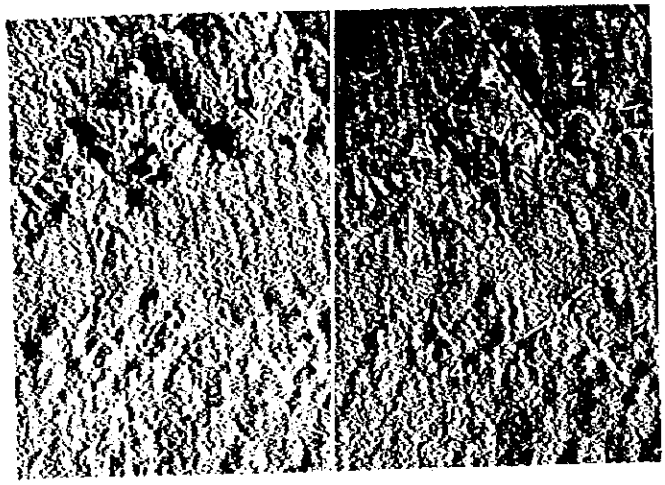

The lower Tertiary Borelis limestone (3) is a cherty, dense rock underlain by Upper and Lower Miocene sandstone (1,2). The siliceous Borelis limestone resembles sandstone in its morphologic appearance (1), but has poorer vegetation. Limestone (4) is the Klasafet Formation, an uplifted Pleistocene coral terrace. It has a nearly horizontal attitude and lies unconformally on 3, which is tilted (arrows). The Klasafet limestone shows pinacled surface on tropical Karst. (Vogelkop, Hollands New Guinea)

Types of folds (*Tipos de Plegados*)

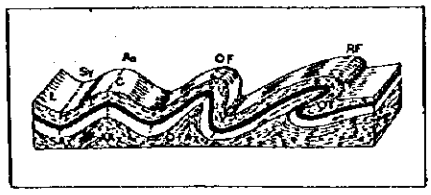

The type depends on the intensity of tectonic pressure. An is an anticline, with crest C and anticlinal axis, AAx. The two slopes are called limbs or flanks (L). The syncline (Sy) and its axis (SAx) indicate that the structure is symmetric. When the axial plane (O-FAx) is tilted, an assymetric or overfold, will result (Of). Continuous tectonic pressure will result in a recumbent or overturned fold (RF). This fold is usually connected with an overthrust (O-T) fault. Recumbent folds may become covers or nappes in intensively folded mountanaous areas.

Block diagram of an anticlinal mountain and a synclinal valley.

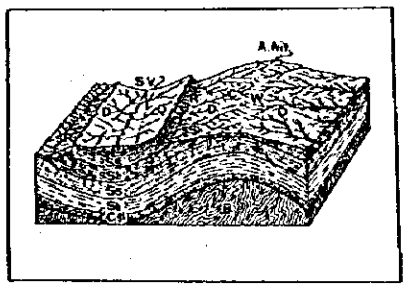

The anticline (A.Mt) forms a ridge. A thick sandstone bed (Ss2) is overlain by a sandy shale (sSh). Consequent drainage C of sandy shale character forms dipslopes (D) which however do not conform with Ss2 below. The watershed W, however, follows the axis of the structure. The synclinal valley (S.V.) is formed by sandstone Ss1. It forms a through with dipslopes (D) and alluvial fill (A). The shale at the left shows a strike controlled strato subsequent river (sR). At the center, stream sR follows the scarp in a similar sense. The tributaries from the anticline are resequent streams ; the steep short gullies from the scarp obsequents (O). Cgl is a base conglomerate ; B is base rock.

Faulting, faceting and dipsloping.

A sandstone formation Ss makes contact with a homogeneous tuff-shale formation (T-Sh). Dipslopes (arrows) show uniform character, similar shape, inclination and direction of dip. The facets (f) developed along fault planes are different in shape, inclination, and direction of the sloping. Ladle-shaped symbols mark direction of fault plane tilt. At X are dipslopes of a sandstone bed overlain by shale. (Carpathian Mountains)

Folding

Landform

Landform

Hills

Landform

Landform

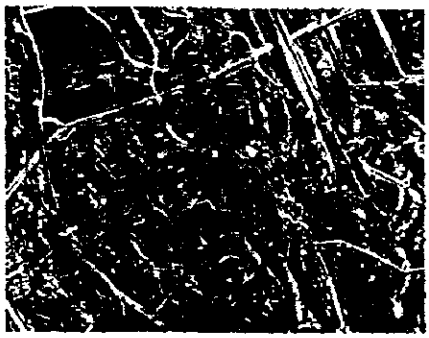

Urbanized Area Tokyo, Japan

Mountainous Area

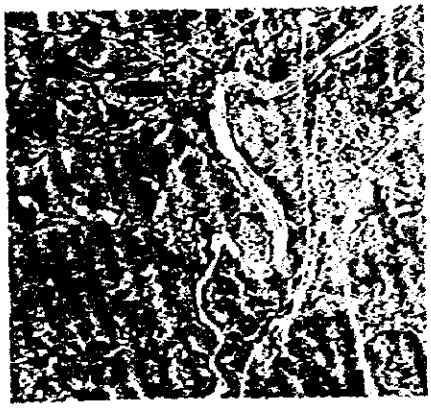

Terrace

Landform

Stratovolcano, Mts. Fuji, Japan

Landform

Monogenetic Pyroclastic Cone

Landform

Rock Glacier , Nepal

Probale lithology

Oblique view of a faulted structure with steep attitudes

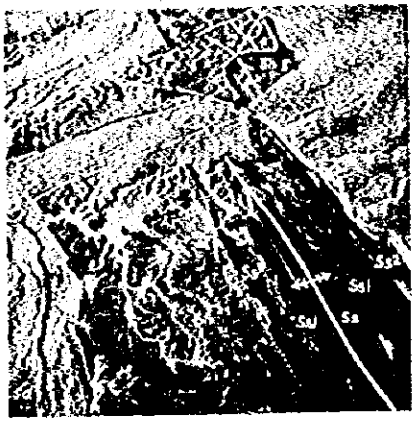

The Sc sandstone in the core is dark brown and shows as dark elongated smooth ridges without surface drainage. Sst wedges out somewhat along the right flank. Greater distance of Sc2 from axial part indicates assymetry. Sh is a shale area well recognizable by its dendritic drainage. Sd is shift or losse sand which shows always in a light tone in arid areas like this. R, R1 are strike controlled braided river beds, sandfilled, with some scanty vegetation. At A is a granular alluvial fill similar to R1. Rather strong faulting by F-F has displaced the axis of the structure. F3 and F form a cross graben ; F2 an oblique fault ; Af an alluvial fan. (North Africa, Sahara)

Alignment of sinkholes

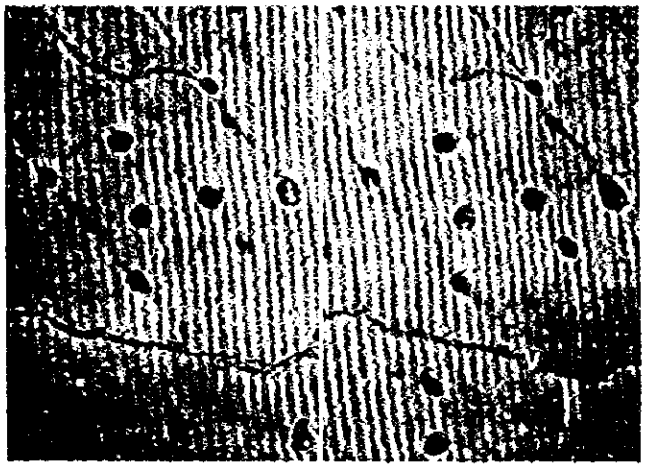

The relation between faulting or jointing and sinkhole forming is visible. Slightly darker lines are dissolved cracks in this horizontal limestone table. The straight wadi (V) is fracture-controlled. Sinkholes (X-X) are at cross-point of dislocation lines. Dark spots in sinks are vegetations. (Chott el Chergui, North Africa)

Schists in arid climate

The schist (Sc) has a dark tone and steep attitude. The banding is well developed and visible on this oblique photograph. The apparent foliation, however, is mainly due to sand filled low depressions and trenches between more resistant ridges. In beds with such steep attitudes, faulting becomes indistinctive. Discontinuity of this schist belt discloses the fault pattern. At X oblique faults (Fo) are cut by longitudinal fault (F). Longitudinal fault (F) disclose obliques (Fo) which are the older. S-S is sand. (Nafud Dahi, Arabia)

On an area in a rainforest, trees of different height and type indicate a plunging anticline

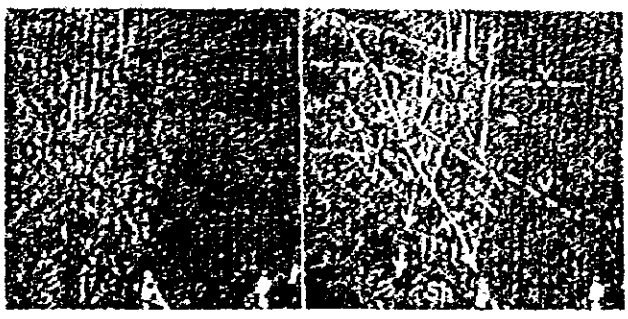

The core of the structure supports a lower tree growth with lighter canopies than the surrounding lowland.
At the flanks and on the plain, trees are higher and darker. Along lines V-V which are fracture lines, trees are highest with darkest canopies. In spite of dense plant cover, details of structure can be plotted (arrows). Fault tectonics and hard formations can be followed.
Even a lithologic conclusion can be made at Sh, where dendritic drainage pattern indicate a shale. At right bottom are cultivated clearings. (Mara District, Venezuela)

Alignment of vegetation on a gravel sand terrace (T,T') shows structural conditions of the underground

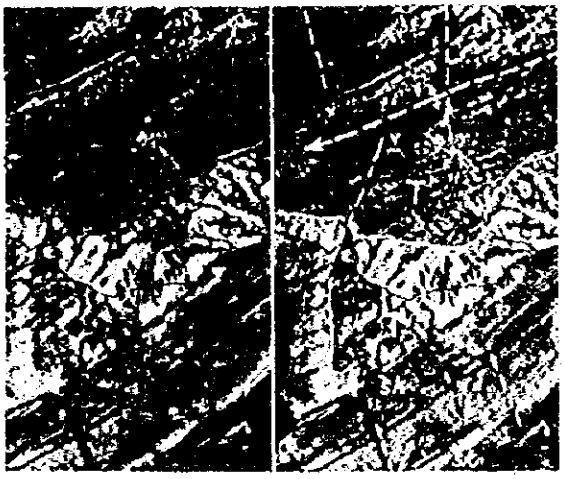

The calcareous Niobrara Formation at the lower half of the stereo, is indicated by infiltration hole rows (Skr) at the bottom. The strike of beds shows through the gravel terrace. Sinkhole (sk) on (T) is indicative for calcareous formation. Under T', a sandstone-shale formation causes alignment of sage brush and grass. The lighter low vegetation thrives on sandy ground; the darker on clayey ground. Note keybed at X-X. At Y, beds show banding and arching. The antiklinal axis is tentative. (Sheep Mountain, Jackson Cy., Colorado)

Dip Faulted Sandstone Shale Complex

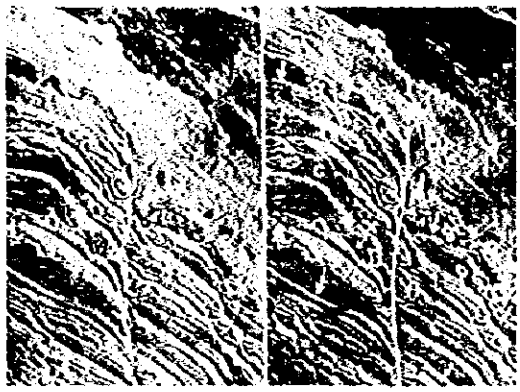

Since dipslopes with low grade attitudes show cross or transversal faulting more distinctly than steeper ones, displacement of beds a,b,c along watergap W can be readily seen. Faultplane cuts the flank (indented line) of an anticline obliquely. At X-X direction of dip turns to the left. The upthrown block (U) is at the right part of the photograph, the downthrown (D) at the left. Arrows mark the dip direction of the sandstone beds. Af is an alluvial fan. Fault data are calculable from dip of beds and distances. (Southern Sahara)

Qurtzite, Quartzite schist in contact with granite.

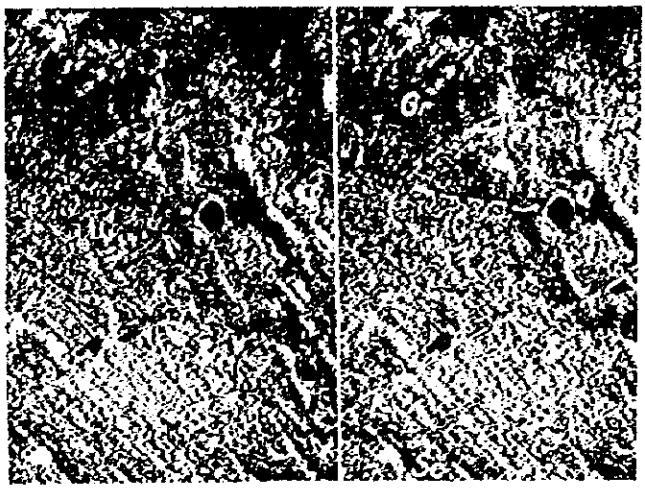

Quartzite (Q) and quartzite schist (Sc) in contact with granite (Gr). The light tone is indicative for metamorphics rich in silica. The thick quartzite (Q) is resistant and forms ridges. Sc is thinner bedded, has alternate mica schist and greenstones. The lakes are glacial. Alignment of vegetation is visible on Sc and is assosiated with the different composition of rock. On Q is a spotty tree vegetation and closed forest on Gr. (Park Range Colorado)

Types of schist in arid climate.

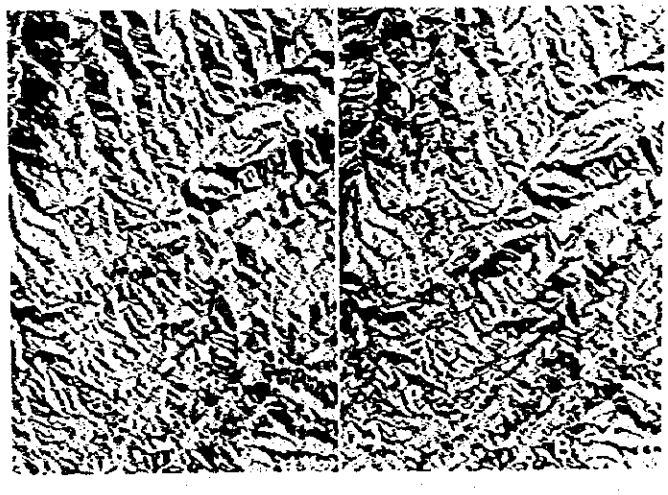

Three types can be distingished. The phyllitic type is rather dark with a close-spaced drainage, indicating lamination at P. Ther is a gradual lateral transition at X between phyllites (mica schist) (P) and quartz schist (Q). Note difference of drainage pattern and forms between P and Q. At B are banded schists with light and dark gray bands. They show the altitude of the schist complex. This is near vertical at B and about 40-50 degrees at B1. T is a remnant of an Pleistocene abrasion terrace with quartzite boulders laying on the surface. (Hlescas Mountains, Sechura, North Peru)

Succession on Miocene andesite lavas and agglomerate in humid climate

There are three lava sheets (Lv, Lv2 and Lv3) covering each other. No flow structures are visible because of advanced weathering.
Lv3 is the oldest, covered by a layer of agglomerates (bombs, lapilli, tuffs) marked with Agl. This is covered by Lv2 which is turn covered by the youngest Lv1. No surface drainage develops on the flows and agglomerates in spite of the tilted position of the beds. At Agl, a few infiltration centers can be seen, similar to sinkholes. The surface is uneven undulating on the lavas. Forest (Fo), low forest (Lf) and shrub (Sb) follow the aquifers. Lavas are covered by grass (Gr).(Transylvania Mountains)

Basalt flow in arid climate

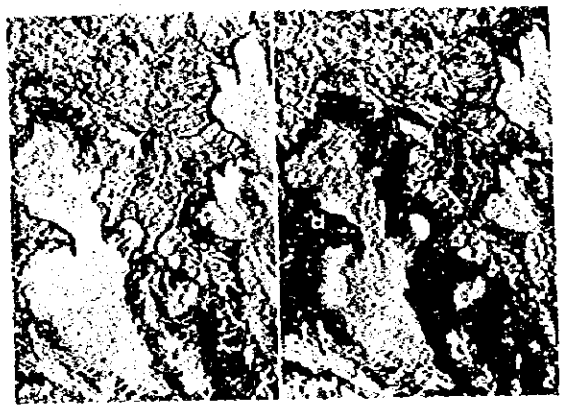

Three lava flows (1,2,3) coming from a nearby vent (near 3, bottom) show a basalt flow topography.
No surface drainage developed on the sheet. Rain seeps through coloumnar cracks and joints (cl). There are a few spotty infiltration centers (sp) similar to those found on fluvial terraces in arid climate. The older flows (1,2) are bleached on the surface due to weathering but the steep walls and the youngest flow 3 have a dark tone. Arrows shows the direction of the flows. The basalt sheet covers a near vertical schist complex. (New Mexico)

Ridge of dacite, an intermediate lava

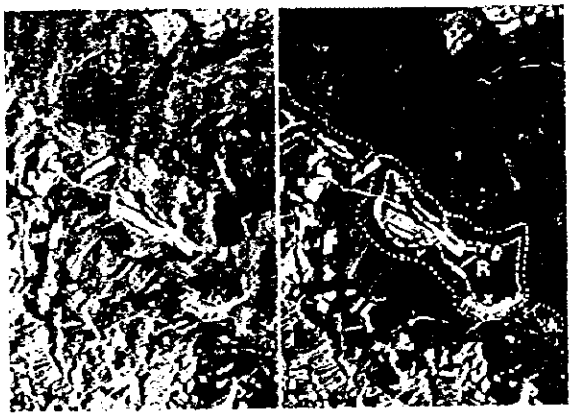

This light gray effusive contains quartz and much feldspar. Rithe tone of the rock visible at X) forms a flat topped ridge with steep slopes. Surface drainage developed along fractures. This type of eruption is an example of a split eruption, through the rather tough lava did not form a cover like basalt often does. (Transylvania)

Semi-metamorphic Mesozoic andesitic tuff and agglomerate

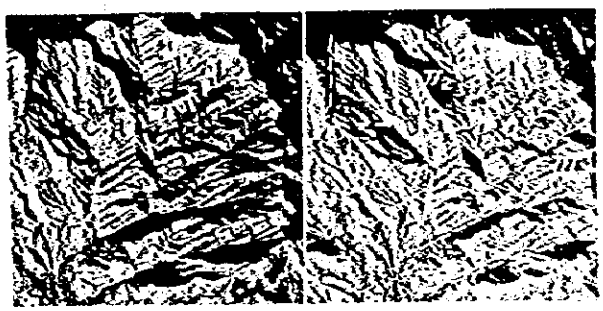

This greenish gray lower Cretaceous extrusive underwent strong tectonic pressure, mainly fracturing. It resembles a schist with its intricate drainage. The general appearance is that of near vertical attitude.
Field observation showed that the tuff complex is near horizontal, indicated on the photo by boundary between coarse pyroclastics (*Ifp*) and finer ones (*Ift*). (Rojada Mts. Sechua, Peru)

Basic igneous intrusive body with radial drainage pattern

A basic igneous intrusive body at B. Radial drainage indicated by arrows. Surrounding schists (Sc) show subparallel to dendritic pattern along schistosity. Both are dark-toned, hence there is little contrast between Sc and B. F-F are fault controlled drainage lines. White spotted areas (X) are quartzite lag-blocks and gravels. Cg is a conglomeratic sandstone overlapping Sc. At Sh are soft shales and sands. (Sechura, Peru)

Biohermal type limestone interbedded in schists

Jurocretaceous reef limestone, locally called *mogotes*, this is a biohermal type interbedded in schists (Sc). The attitude of the lenticular limestone mass (L) is steep, near vertical. Sinkholes are oval shaped. At R is residual red clay. At Sl are slates. (Organos Mountains, West Cuba)

Contact between Granite and schist

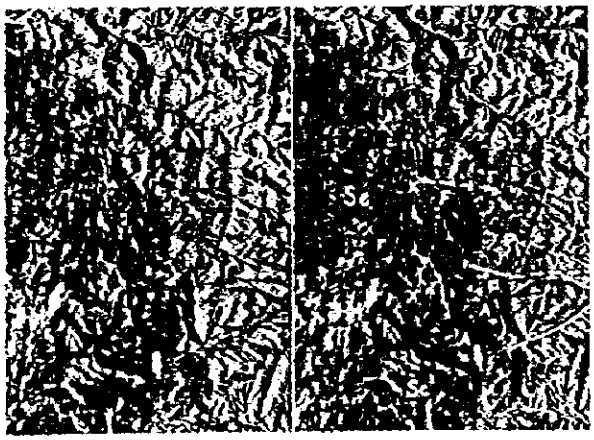

The Jurassic granite (Gr) has a lighter tone than the dark, Carboniferous schist (Sc). The contact can be plotted along the tone difference. This results in outline of faulting along F-F. This abrupt change in contact outline interrupts the otherwise smooth curved boundary. The granite shows a tree-like drainage pattern with *pincers* at P-P. The principal fault controlled drainage lines are marked. At A-A are aplitic dikes in the schist. Foliation of the schist complex is at Scl. At X-X are quartzite inlays in the schist with a lighter tone. At T is an abrasion terrace with large quartzite blocks on the surface causing lighter tone. (Illescas Mountains , Sechura, Peru)

Folding (plege)

Anticline

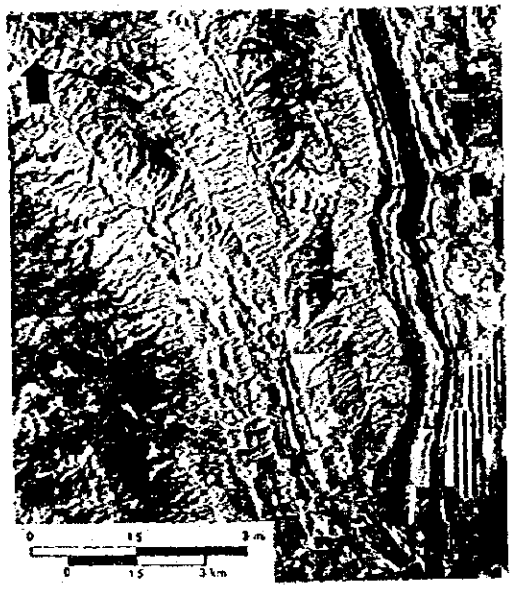

Color Infrared NASA Airphoto of Milner Mountain, Colorado
(North is at the top).

Anticline

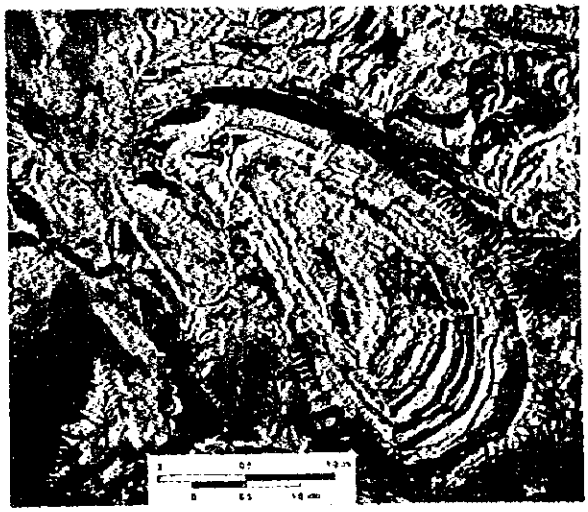

Circle Ridge Anticline, Wind river Basin, Wyoming.
(North is at to of photo)

Anticline, Fault

Landsat Thematic Mapper Image over the Hodna Field Area, Algeria

Fracture (Fractura)

Fault planes and facets in sandy shale area.

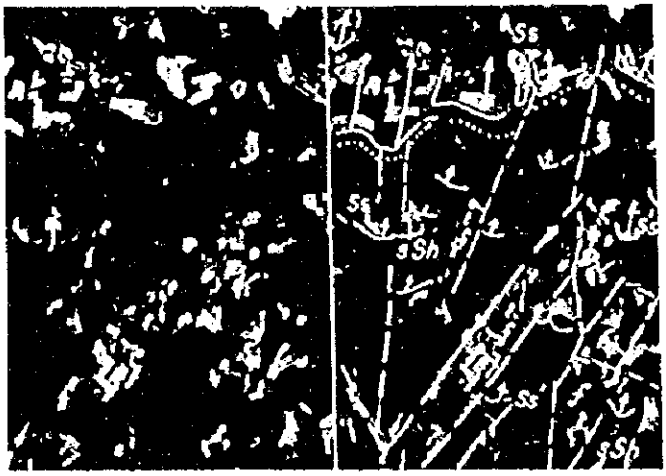

The oligocene sandy shale complex (sSh) has a few thin sandstone beds (Ssl), sufficient to evaluate the strike of the formation. The capping Miocene sandstone beds Ss form good dipslopes. The boundary indicates cross faulting which extends into the shales. At f-f, long, rathe even slopes developed. They have different inclination and direction.
The opposite sides of the fault-controlled valleys are deeper incised than the facets (f) which are not yet eroded deeply. (Transylvania)

Fractured granite mass with radial drainage

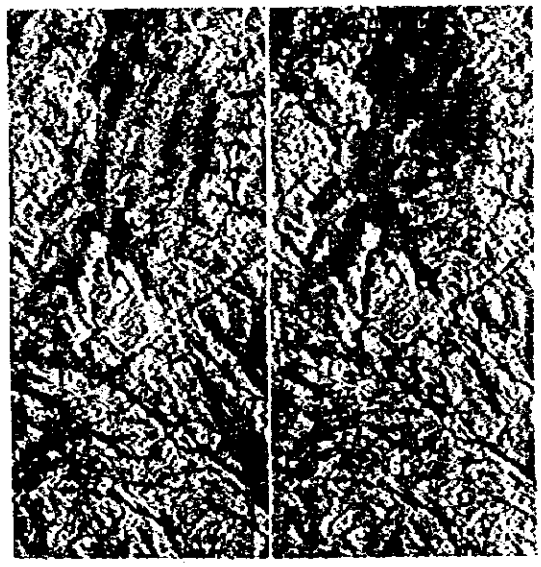

The Sherman Granite of Colorado shows a generally radial drainage, which is fracture controlled and therefore angular. The fault pattern causes trenches F and F1 marked by tree alignments. G1 is a massive granite with rounded forms but G2 is a strongly compressed variety, approching gneiss.
The forms are sharp, lamellated and resemble more schist than granite. This lamellation is caused by pegmatite dikes, which have greater resistance. (North park, Colorado)

Basalt effusion in arid climate

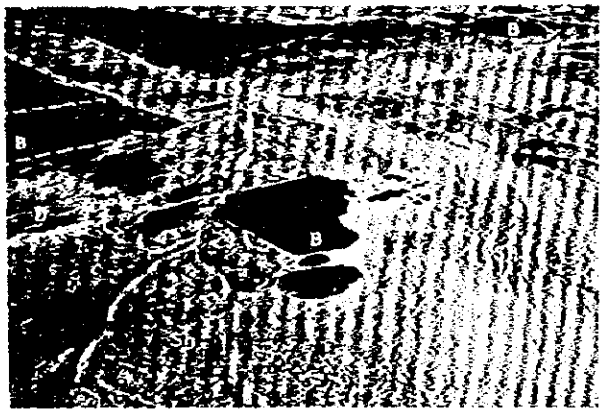

Injected into sediments (Sh), (S) the black fluid basalt lava reached the surface forming covers (B). The eruption took place along fissures, the system of cut-faults marked by dashed lines. Dikes (D) accentuate the fault system the eruption followed.
This is a split eruption type with sheet and dyke forms. The sediments are mainly shales in great part removed. Note typical silt-shale drainage pattern at bottom. Basalt with their contrasting dark tone are good tectonic indicators in arid regions. Note close spaced tree-like drainage pattern in silty shales (Sh) and no pattern in sand (S). (Central Arabia)

Strike-controlled sinkholes

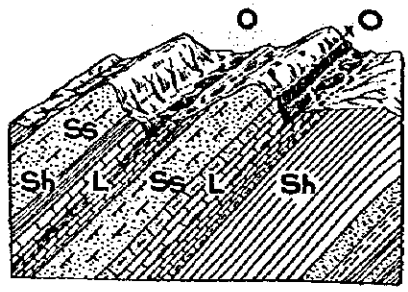

Oval sinks (O) develop on tilted interbedded limestone beds (L). Sandstones (Ss) are permeable but insoluble,shales (Sh) are impervious. At X is a jagged scarp of arenaceous, lesssoluble limestone.

Fault-controlled sinkholes

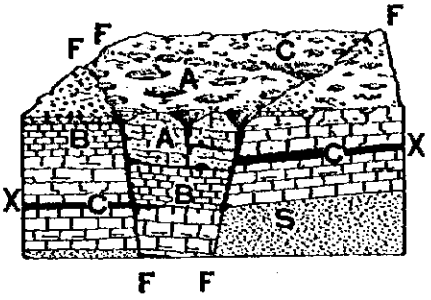

Sinkholes show alignment and are deepest and broadest at cross-point of dislocations. Three types of limestones have large (A), medium (C), and small (B) sinks. At X is an impervious beds ; S, sand ; F-F, fault planes. Water drains into sand, follows enlarged fissures and bedding planes in limestone.

Lineament (Interpretation)

Lineament and foldings develops on the quartzite (ridge), and metapelite (valley) Near Alwar, Rajasthan

Lineament

Lineament and foldings develops on the quartzite (ridge), and metapelite (valley) Near Alwar, Rajasthan

Thrust Fault

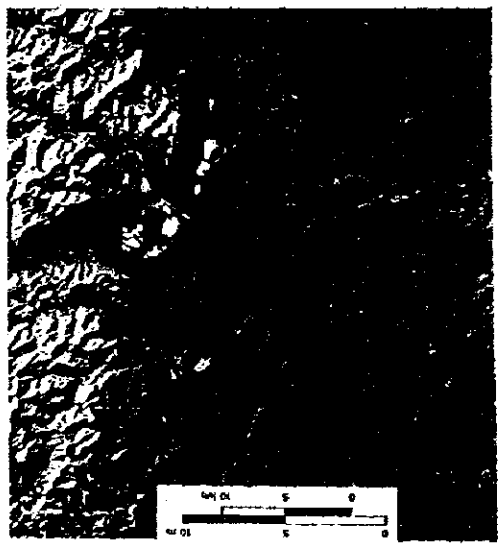

The transition from imbricate ridges to folds (at arrow) marks the frontal thrust of the Brooks Range at the Itkhak River, Alaska. Thrusting here is from south or southeast to north or northeast. (by Landsat MSS image)

Fault

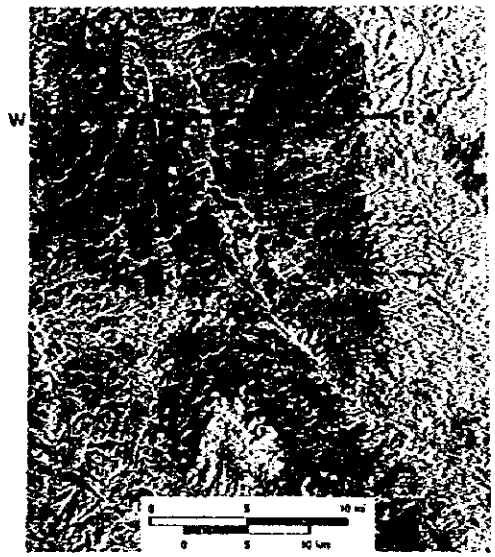

Landsat MSS color infrared images of the Rampart Range, Colorado, from Pikes Peak to Castle Rock. Arrows indicate faults parallel to the mountain front.

Fault Control

Vegetation (red) is alingned along springs, which in turn are controlled by faulting along the margins of spring valley, Nevada. Also note the paleo-shorelines at the north end of the valley.

Basalt Dyke Intrudes the Tertiary

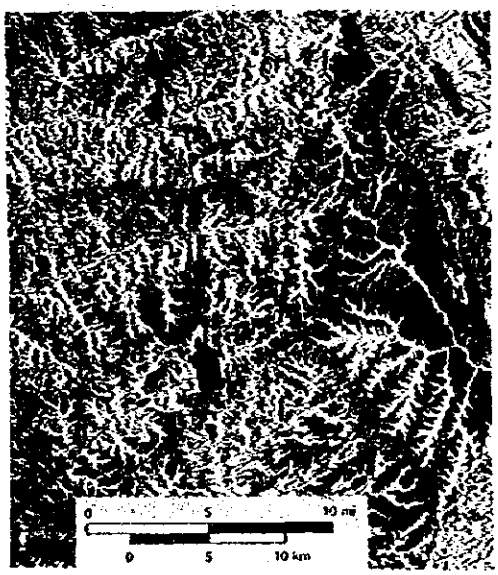

Basaltic dyke (arrow) intrudes the Tertiary in the northeastern San Juan basin, New Mexico. Intrusion was Contemporaneous with jointing.

Tectonic Line

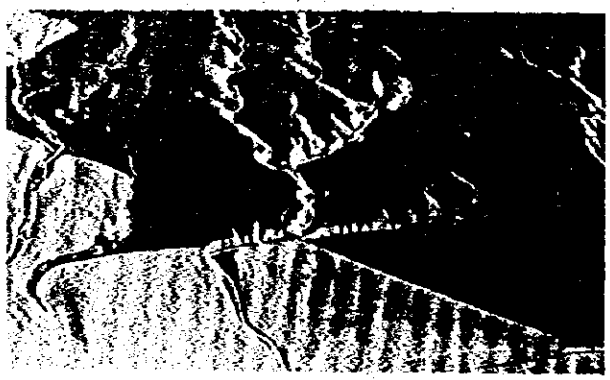

San Andreas Fault

Tectonic Line

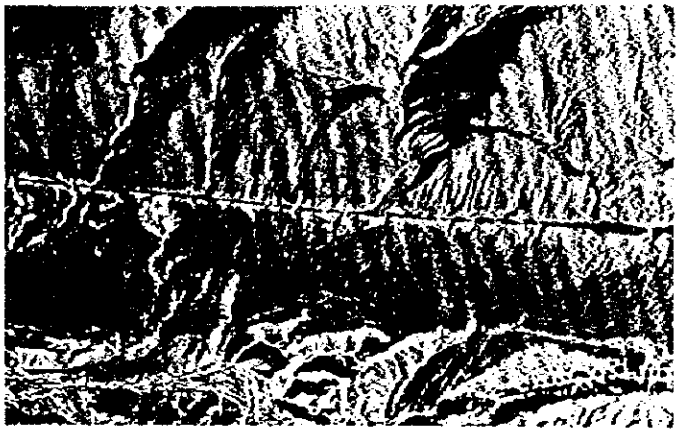

Garlock Fault, Transverse Mts, California

Mapping

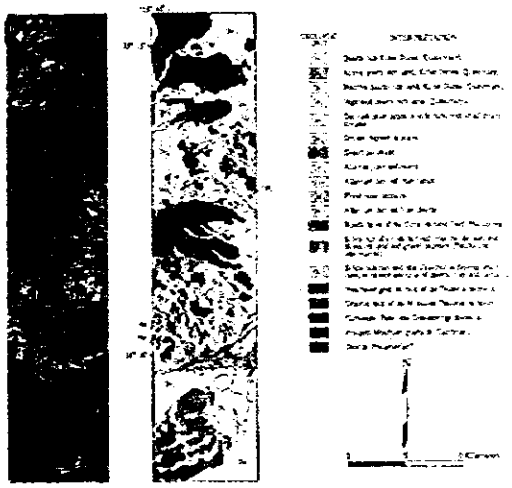

The surficial map was derived from the image. In general, quartz rich rocks are red ; alluvium is reddish pink (older) to red with a blue cast (younger) ; vegetation is yellow ; carbonates range from bright green to yellow ; quartzites are orange ; and basalts are dark blue-green.
(by Thermal Infrared Multispectral Scanner (TIMS), image of part of the Mojave Desert near Kelso, California).

References (*Referencia*)

Barry S. Siegal , Alain R. Gillespie (1979)
Remote Sensing in Geology
John wiley & Sons New York chichester Brisbane Toront

Horst F. von Bandat, PH.D. (1962)
Aerogeology
Gulf Publishing Company Houston,Texas

Vitor C. Miller, Calvin F. Miller(1961)
Photogeology
McGraw-Hill Book Company Inc. New York

Keenan Lee, Daniel H. Knepper, Jr.,et al (1989)
Remote sensing in exploration geology
Field Trip Guidbook T182
American Geophysical Union, Washington, D.C.
2000 Florida Avenue N.W., Washington D.C. 20009

Christopher Legg (1995)
Remote Sensing and geographic Information Systems
(Geological Mapping, Mineral Exploration and Mining)
Wiley-Praxis Series in Remote Sensing
Praxis Publishing Ltd. The White House Eastergate, Chichester
West Sussex , PO206UR, England

Robert K. Vincent (1997)
Fundamentals of Geological and Environmental Remote Sensing
Prentice-Hall, Inc. Simon & Schuster / A Viacom Company
Upper Saddle River, NJ 07458

Ravi P. Gupta (1991)
Remote Sensing Geology
Springer-Verlag Berlin Heidelberg, Printed in Germany

Gary L. Prost (1994)
Remote Sensing for Geologist
(A Guide to Image Interpretation)
Overseas Publishers Association Amsterdam B.V.
published in the Netherland Under License by Gordon and Breach Science Publishers.

H.V.d.Meer Mohr (1986)
Hand-Out Photo Interpretation for Geology
International Institute for Aerospace Survey and Earth Sciences
Enschede, Netherland

研修完了証書の見本

Subsecretaría de Minería de la Nación

Servicio Geológico Minero Argentino

• SEGEMAR •

Agencia de Cooperación Internacional del Japón

• JICA •

Agencia de Minería Metálica del Japón

• MMAJ •

Certificamos que .....

ha participado del Curso sobre ***"Análisis de Sensores Remotos, con especial énfasis en interpretación geológica de imágenes satelitales con propósitos de exploración."***

Dictado por el Profesor Masataka Ochi, con una duración de 24 horas,

13 al 16 de octubre de 1998 • San Juan, República Argentina

Dr. Daniel Meilán
Subsecretario de Minería

大澤尚正

Lic. Naomasa Osawa
Representante Residente de JICA en Argentina